View metadata, citation and similar papers at core.ac.uk

brought to you by CORE

provided by University of Tennessee, Knoxville: Trace

University of Tennessee, Knoxville
Trace: Tennessee Research and Creative Exchange

Masters Theses

Graduate School

8-2010

Influenza-specific B cell responses in HLA-DR1 transgenic mice

Lifang Huan
University of Tennessee - Knoxville, lhuan@utk.edu

Recommended Citation
Huan, Lifang, "Influenza-specific B cell responses in HLA-DR1 transgenic mice. " Master's Thesis, University of Tennessee, 2010.
https://trace.tennessee.edu/utk_gradthes/718

This Thesis is brought to you for free and open access by the Graduate School at Trace: Tennessee Research and Creative Exchange. It has been accepted for inclusion in Masters Theses by an authorized administrator of Trace: Tennessee Research and Creative Exchange. For more information, please contact trace@utk.edu.

To the Graduate Council:

I am submitting herewith a thesis written by Lifang Huan entitled "Influenza-specific B cell responses in HLA-DR1 transgenic mice." I have examined the final electronic copy of this thesis for form and content and recommend that it be accepted in partial fulfillment of the requirements for the degree of Master of Science, with a major in Microbiology.

Mark Y. Sangster, Major Professor

We have read this thesis and recommend its acceptance:

Thandi Onami, Tim E. Sparer

Accepted for the Council:
Dixie L. Thompson

Vice Provost and Dean of the Graduate School

(Original signatures are on file with official student records.)

To the Graduate Council:

I am submitting herewith a thesis written by Lifang Huan entitled "Influenza-specific B cell responses in HLA-DR1 transgenic mice." I have examined the final electronic copy of this thesis for form and content and recommend that it be accepted in partial fulfillment of the requirements for the degree of Master of Science, with a major in Microbiology.

Mark Y. Sangster

Major Professor

We have read this thesis
and recommend its acceptance:

Thandi Onami

Tim E. Sparer

Accepted for the Council:

Carolyn R. Hodges

Vice Provost and Dean
Of the Graduate School

(Original signatures are on file with official student records.)

Influenza-specific B cell responses in HLA-DR1 transgenic mice

A Thesis Presented for

The Master of Science

Degree

The University of Tennessee, Knoxville

Lifang Huan

August 2010

ACKNOWLEDGEMENTS

It is my pleasure to thank many people who made this thesis possible. Foremost, I would like to express my sincere gratitude to my advisor Dr. Mark Sangster for his continuous support for my study and research, and for his patience, motivation, enthusiasm and immense knowledge. His guidance helped me in my research and writing of this thesis all the time. In addition, he was always accessible and willing to help his students. As a result, research life became smooth and rewarding for me.

I gratefully acknowledge my committee members, Dr. Thandi Onami and Dr. Tim Sparer, for their time and helpful guidance.

I would also like to thank my lab buddies: Hye Mee Joo and Aarthi Sundararajan for their friendship and help in the past three years. All other folks, including Junwei Zeng and John Harp, had inspired me in my research and life through our interactions in the lab.

My deepest gratitude goes to my parents who are always beside me and encourage me to go for my dream. I am eternally grateful for their support and prayers.

Last but not the least, I greatly express my appreciation to my husband Rick Chen for his support, love and persistent confidence in me. Thank you for putting up with me through this process.

ABSTRACT

HLA-DR1 transgenic (DR1 Tg) mice provide a model for evaluating the breadth and specificity of CD4 T cell responses that may develop in humans following influenza infection or vaccination. Recent studies identified a tremendously broad HLA-DR1-restricted CD4 T cell responses in DR1 Tg mice infected intranasally with influenza A/New Caledonia/20/99 (NC). In this study, our goals were to characterize B cell responses after NC infection in DR1 Tg mice and establish the correlation between B cell responses and CD4 T cell responses in this system. Influenza-specific B cell responses following virus administration were analyzed in DR1 Tg mice and in the genetically matched *H-2*^{b} strain C57BL/10J (B10).

Following intranasal (i.n.) NC infection, B cell responses in B10 mice featured strong IgG2b and IgG2c production and were typical of previously described B cell responses to a variety of mouse-adapted influenza strains. In contrast, B cell responses in DR1 Tg mice followed delayed kinetics and were strongly skewed to IgG1 production, suggesting the Th2 polarization of CD4 T cell responses. The different antibody isotype profile in DR1 Tg mice compared to B10 mice was evident in antibody secreting cells (ASCs) frequencies and in circulating Abs levels. Surprisingly, although DR1 Tg mice had lower influenza-specific Abs levels, they exhibited higher neutralizing Abs titers early in the response.

B cell responses following intranasal infection of influenza A/Puerto Rico/8/1934 (PR8) or intramuscular vaccination of inactivated NC in DR1 Tg mice were different from the observed IgG1 bias after i.n. NC infection. After i.n. PR8 infection, B cell responses were characterized by predominant IgM/IgG3 production, which was similar in DR1 Tg mice and

B10 mice. Additionally, following intramuscular administration of inactivated NC, B cell responses were skewed towards IgG2c production in both DR1 Tg mice and B10 mice, suggesting the Th1 polarization of CD4 T cell responses. A mechanistic understanding of IgG1/Th2 biased B cell responses and better neutralizing Abs production in DR1 Tg mice following i.n. NC infection may have implications for the optimal control of influenza infection.

TABLE OF CONTENTS

LIST OF FIGURES

ABBREVIATIONS

ASC……..... Antibody secreting cell

Ab…….. Antibody

APC……. Antigen presentation cell

BCM……. B cell medium

BM…….. Bone marrow

BPL……. β-propiolactone

BSA……. Bovine serum albumin

CLN……. Cervical lymph node

CPE……. Cytopathogenic effect

FBS……..…….. Fetal bovine serum

GC…….. Germinal center

HEV……...…… High endothelial venule

HLA……. Human leukocyte antigen

IliLN……..……. Iliac lymph node

ILN……..…… Inguinal lymph node

i.n..…….. Intranasal

i.m..……. Intramuscular

MHV-68…….. Murine herpesvirus 68

MLN…….……..…… Mediastinal lymph node

PLN..……... Popliteal lymph node

RDE……. Receptor destroy enzyme

VGM…… Virus growth medium

CHAPTER 1

INTRODUCTION

I. Overview of influenza viruses

The influenza virus is one of the most important human respiratory pathogens and attacks the host respiratory tract mucosa, causing seasonal outbreaks, endemic infections and periodic pandemics [1]. Influenza viruses are enveloped viruses belonging to the family Orthomyxoviridae and contain a negative, segmented, single-stranded RNA genome [2]. Based on antigenic differences of core proteins, nucleoprotein (NP) and matrix protein (M), influenza viruses are divided into types A, B and C [3]. Based on antigenic differences of two surface glycoproteins, hemagglutinin (HA) and neuraminidase (NA), type A viruses are further subdivided into subtypes [3]. Currently, 16 HA (H1-H16) and 9 NA (N1-N9) subtypes have been identified in influenza A viruses [4].

Influenza A viruses have been isolated from various animals, including birds, pigs, horses, humans and sea mammals, whereas type B and C influenza viruses are predominantly found in humans [5]. Influenza A and B viruses cause annual epidemics or local outbreaks of influenza in humans [1]. All different subtypes of influenza A can be found in avian hosts, and therefore aquatic birds are thought to be the natural reservoir of influenza A viruses [6]. However, since the last century, only H1N1, H2N2, and H3N2 subtypes have been associated with widespread epidemics in humans [2]. Although a number of avian influenza viruses (H5N1, H9N2, and H7N7) have crossed the species barrier and directly infected humans, they still have not developed the capacity for efficient human-to-human transmission [3].

Genetics of the influenza A virus

The genome of influenza A viruses (Fig. 1) contains eight single-stranded, negative-sense RNA segments and codes for at least 10 proteins in vivo by using different reading frames and alternative RNA splicing [3]. The virus particle has a lipid envelope that is derived from the host cell during budding through the cell membrane [5]. Three proteins are embedded in the lipid bilayer: the rod-shaped HA, the mushroom-shaped NA, and the matrix protein 2 (M2) [3]. The matrix protein 1 (M1) is the most abundant protein in the virus particle and locates right below the lipid bilayer [7, 8]. Genomic RNA segments are encapsulated with the nucleoprotein (NP) and are associated with three RNA polymerase proteins (PB1, PB2, PA) to form ribonucleoprotein (RNP) complex [3, 9]. The virus also encodes nonstructural proteins NS1 and NS2. NS1 counteracts the type I interferon antiviral program of host cells by sequestering viral RNAs from intracellular receptors; NS2, also referred to as the nuclear export protein (NEP), is involved in the process of nuclear export of RNPs and viral assembly [10].

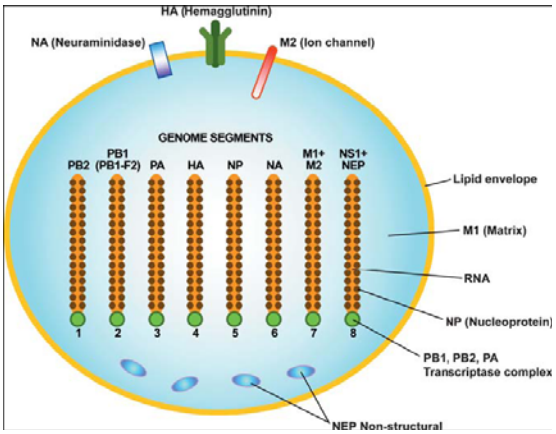

Figure 1. Structure of the influenza A virus [7]

Two major surface glycoproteins, HA and NA, are the most important targets of neutralizing Abs during influenza infection [1, 11]. HA is responsible for the binding of viruses to sialic acid-containing receptors and the membrane fusion between the virus and the host, resulting in the release of viral RNPs into host cells [8]. NA cleaves sialic acid residues of cellular receptors and releases new viruses [3].

Pathogenesis of the influenza A virus

Influenza is an acute and contagious respiratory disease, characterized by the sudden onset of systemic and respiratory symptoms including fever, headache, cough, sore throat and rhinitis etc. [3]. All influenza A subtypes are carried in the gastrointestinal tract of wild birds asymptomatically, but may cause diseases in domestic birds and mammals [12].

Influenza viruses are constantly undergoing antigenic changes to escape the host adaptive immunity in two ways: antigenic shift and antigenic drift [3]. Due to the segmented viral genome, influenza viruses can easily reassort segments from different strains in a doubly infected host [3]. The reassortment will result in the emergence of a new subtype with novel antigenic properties, referred to as antigenic shift [3]. Antigenic shift can also occur when an avian strain is directly transmitted to humans without reassortment [13]. Antigenic shift happens at infrequent and unpredictable intervals. Since a large proportion of human populations have little or no immunity to the new subtype and antibodies against the previously circulating strain do not cross-react with it, the new subtype possesses the potential to cause a global pandemic [3, 8]. Viruses causing the pandemics of 1957 and 1968 were derived from the reassortment of avian and human viruses [14, 15].

Antigenic drift results from the continuous accumulation of minor genetic mutations in all gene segments, mostly in surface glycoproteins HA and NA [3]. Viral RNA-dependent RNA polymerase complex lacks proofreading abilities, resulting in high rates of point mutations (~ $1/10^4$ base per replication cycle) during genome replication [16]. Variant strains of the same subtype contribute to annual epidemics or local outbreaks of influenza.

The binding specificity of HA for host cells is thought to be a major determinant of whether an influenza strain can infect a host [7]. An important difference between avian and human viruses is their binding preferences for specific sialic acid linkages on host cells [2]. Most avian influenza viruses preferentially bind to α-2,3 sialic acid linkages, whereas human strains preferentially bind to α-2,6 sialic acid linkages [17, 18]. Upper respiratory tract epithelial cells of birds and human preferentially express virus receptors with α-2,3 sialic acid linkages and α-2,6 sialic acid linkages, respectively, whereas respiratory epithelial cells of pigs express receptors with both α-2,3 and α-2,6 sialic acid linkages [19].

The receptor binding specificity and expression pattern has led to the hypothesis that pigs serve as a “mixing vessel” which facilitates antigenic shift [15, 19]. When pigs are infected with human and avian viruses simultaneously, reassortment may occur to give rise to a new pandemic strain with efficient human-to-human transmission capacity [7]. The receptor binding specificity and expression pattern also accounts for the usual restriction of infection by avian strains to birds and pigs but not humans [2]. However, research showed that a human virus A/New Caledonia/20/99 was able to replicate effectively in mice lacking α-2,6

sialic acid linkages, indicating that this restriction was not totally absolute [20].

HA is synthesized as an HA0 precursor, which needs to be cleaved into two subunits HA1 and HA2 by host proteases at a conserved arginine residue [7, 9]. HA of highly pathogenic avian influenza (HPAI) has a series of basic amino acids at the cleavage site enabling HA to be cleaved by ubiquitous proteases, which facilitates systemic infection and spread of the virus [21]. Therefore, HA cleavability is considered as another major determinant of virus pathogenicity.

Other gene segments can also contribute to the pathogenicity of influenza viruses. It is still not clear what resulted in the extreme virulence of the extinguished 1918 pandemic strain. Research based on the successful reconstruction of this strain showed that HA, NA, and PB1 genes were responsible for the high replication efficiency of the reconstructed strain observed in mouse and human airway cells [22]. PB1 gene probably played a crucial role in the 1918 virus virulence [22]. PB2 gene appeared to contribute to the efficient transmission of viruses by allowing enhanced replication at a lower temperature in the airway of mammals [23].

Epidemiology

Influenza epidemics usually occur between November and March in the northern hemisphere and between April and September in the southern hemisphere [2]. Influenza is responsible for over 100,000 hospitalizations and around 20,000 deaths annually in the US [24, 25]. During a pandemic, which usually happens every several decades, the morbidity and mortality increase dramatically.

There were three influenza pandemics in the last century [26]. The 1918-1919 Spanish influenza was caused by a H1N1 strain and killed more that 40 million people [27]. Almost 50% of deaths occurred in an unusually young age group, 20-40-year-olds [28]. A new influenza H2N2 virus was responsible for the 1957 Asian influenza pandemic and was first isolated in Japan in May 1957 [2]. A H3N2 strain caused the third pandemic and was isolated at Hong Kong in 1968 [2]. This strain contained avian HA (H3) and PB1 segments, and shared other segments with the previously circulating H2N2 virus [5].

In late March and early April 2009, an outbreak of H1N1 influenza A virus infection was detected in Mexico, followed by many other countries including the US [29]. The pandemic (H1N1) 2009 influenza A virus is a new reassortant comprising two swine strains, one human strain and one avian strain [26]. Recent data from numerous outbreak sites show that the pandemic (H1N1) 2009 virus is currently the dominant strain circulating in most parts of the world [30].

II. The immune response to influenza viruses

The respiratory tract mucosa is not only the site of influenza infection but also the site of defense against influenza infection in the host [1]. The kinetics study of the influenza A virus showed that infected epithelial cells started to produce viruses 6 hours after infection [31]. The virus titer in the lung usually peaks 2-3 days post-infection, and becomes undetectable around 10 days post-infection [32]. However, the host adaptive immune response needs about one week to develop [32]. Therefore, in order to control virus infection or recover from influenza, both innate and adaptive immune responses should be induced [1].

Innate immunity to influenza viruses

The innate immune response triggered by virus infection functions as the first line of defense to restrict viral spread. The innate system consists of effector cells (such as epithelial cells, NK cells, macrophages, and plasmacytoid dendritic cells), cytokines and chemokines (including IFNs, TNF-α, IL-1, IL-6, IL-12, MIP-1, IP-10), and complements [1, 33]. The recognition of viral RNAs by TLRs induces the production of cytokines and chemokines by infected lung epithelial cells and macrophages [34, 35]. The cytokines and chemokines then contribute to attracting monocytes and T cells from peripheral blood into the site of infection within the first 3 days after infection [34].

Type I IFNs, which are produced by infected epithelial cells, macrophages, and plasmacytoid dendritic cells, are important components of the innate immune response due to their direct antiviral effects [7]. The IFN-α/β response starts within 12 hours after infection and lasts for several days [36]. Type I IFNs influence CD4 differentiation resulting in the development of Th1 effector cells that in turn produce high levels of IFN-γ and IL-2 [37].

Adaptive immunity to influenza viruses

After influenza viruses successfully escape the innate immune response and establish intracellular infection, the adaptive immune system will play a key role in the host defense by detecting and eliminating infected cells [38]. The adaptive immunity is comprised of cell-mediated immune system and humoral immune system.

The cell-mediated immune system, consisting of CD4 T cells and CD8 T cells, is essential for virus clearance during influenza infection [3]. CD8 T cells, also called cytotoxic lymphocytes (CTLs), recognize an antigenic peptide-MHC class I complex through TCRs and become activated [1]. Activated CTLs not only directly lyse infected cells, but also secret pro-inflammatory and anti-viral cytokines, such as IFNs [39]. CD4 T cells recognize antigenic peptide-MHC class II complex on APCs and then differentiate into different subtypes, such as Th1, Th2, Treg, and Th17 [40]. Th1 cells secrete IFN-γ and IL-2, and provide help for CD8 T cells proliferation and IgG2a/IgG2c production by antibody secreting cells (ASCs); Th2 cells secrete IL-4 and IL-5, and help IgA, IgG1 and IgE production by ASCs [34].

The humoral immune system relies on the production of antibodies by B cells to protect against influenza. Virus-specific Abs against HA and NA are thought to be the most protective [32]. Anti-HA Abs neutralize the infectivity of viruses, and anti-NA Abs reduce the release of viruses from infected cells [41]. Abs to the conserved protein M2 are cross-protective among different subtypes, while Abs to the conserved NP and M1 fail to contribute to protection [42, 43]. The secretory IgA (sIgA) produced locally at mucosal sites is the major neutralizing antibody to prevent virus entrance especially at the upper respiratory tract [3].

Long-lived plasma cells and memory B cells also contribute to the protective immune response [44]. They are able to induce rapid recall responses and produce high-affinity antibodies to neutralize viruses, which are important to control the spread of viruses during the early stage of infection [45]. Long-lived plasma cells reside in the bone marrow after infection and constitute the main source of circulating antibodies in serum as well as antibodies at mucosa sites [46]. Memory B cells usually

circulate and disperse to secondary lymphoid organs throughout the body [47]. An analysis of memory B cells induced by influenza infection identified the lung as a non-lymphoid site where memory B cells as well as ASCs preferentially localize [48].

III. B cell activation, proliferation and differentiation

After their generation and maturation in the bone marrow, naïve B cells migrate to the blood and enter secondary lymphoid organs through high endothelial venules (HEVs) in the outer T cell zone and interfollicular regions [49, 50]. B cells then migrate to B cell follicles where they are retained for up to 24 hours to scan for specific antigens [49]. This migration is dependent on the expression of CXCR5 by B cells and its ligand CXCL13 by follicular stromal cells [51]. Inside follicles B cells are highly motile in a “random walk” fashion and search for antigens [52].

So how do antigens get into lymph nodes from outside and where do B cells encounter antigens? Antigens of low molecular weight can freely diffuse into B cell follicles via pores on the floor of subcapsular sinus (SCS) [53]. Antigens can also travel through conduits into B cell follicles [54]. Dendritic cells (DCs) use Fc receptor FcγRIIB to non-degradatively uptake antigens and then migrate to the T cell zone [55]. Therefore newly arriving B cells via HEVs have the chance to encounter antigen-bearing DCs during their migration to B cell follicles [50].

Recently, the use of two-photon microscopy identified the SCS macrophage as another important antigen encounter site within the first few hours of the immune response [56-58]. When antigens entered LNs via lymph flow, SCS macrophages captured immune complexes (ICs), viruses or virus-like particles, and then presented intact antigens to

follicular B cells [59]. Noncognate B cells were observed to capture ICs from SCS macrophages by complement receptor 1 and 2 (CR1/2) and deliver these ICs to follicular dendritic cells (FDCs) within follicles [58]. FDCs as specialized Ag-trapping cells within follicles can retain ICs on their surface and present intact antigens to B cells [59].

After encountering antigens in B cell follicles, B cells recognize and bind to antigens by the B cell receptor (BCR) [60]. The BCR consists of membrane immunoglobulin (mIg) associated with Igα-Igβ heterodimers [61]. Antigens are internalized through binding to BCRs, processed within specific endosomal compartments, and finally presented in complexes with MHC class II molecules [62]. Antigen-engaged B cells then migrate to the B-T boundary where activated T cells also relocate [50]. B cells can be retained there to allow for encountering CD4 helper T cells and forming stable cognate T-B interactions to get essential help signals for further differentiation. Then activated B cells can undergo one of two differentiation pathways: the extrafollicular pathway or the germinal center pathway [63, 64].

In the extrafollicular pathway, activated B cells migrate to sites without T cells and differentiate into plasmablasts [65, 66]. After ~3 days these plasmablasts further differentiate into short-lived plasma cells to secrete antibodies with low affinities [67]. In the germinal center reaction, activated B cells migrate to the center of B cell follicles and proliferate within the FDCs network, resulting in the formation of the germinal center (GC) [64]. The GC is the main site of supporting the antibody affinity maturation and the generation of memory B cells. The dark zone and the light zone are termed in the GC on the basis of their histological appearances [68].

According to a classic model of antibody affinity maturation, B cells in the dark zone, called “centroblasts”, undergo extensive proliferation and somatic hypermutation [68]. Centroblasts then migrate to the light zone and differentiate into smaller “centrocytes” [68]. Centrocytes undergo the selection for high affinity BCRs with the help of FDCs and Follicular helper T (Tfh) cells [68]. FDCs are capable of capturing large amount of intact antigens in the form of ICs [69]. The follicular helper T cell is a subset of activated CD4 T cells [70]. By competing for binding to antigens displayed on the surface of FDCs, B cells with high affinity BCRs are selected [68]. Selected centrocytes then present antigens to Tfh cells through MHC II complex and compete for help signals [70]. B cells that survive and contain high affinity BCRs exit the GC and become high affinity plasma cells or memory B cells [68].

IV. CD4 T cell responses and MHC class II-restricted epitopes study

Naïve CD4 T cells are activated by professional APCs (such as dendritic cells) in the T cell zone of secondary lymphoid organs. Activated T cells are induced to differentiate into Th1 cells by IFN-γ and IL-12, or into Th2 cells by IL-4 [40]. Activated CD4 T cells up-regulate the CD40L expression and secret different cytokines, such as IFN-γ and IL-2 from Th1 cells and IL-4, IL-5 and IL-10 from Th2 cells, to provide help for B cell proliferation and immunoglobulin isotypes switching [71, 72].

APCs process exogenous antigens into small fragments and finally present antigenic peptides in the context of MHC (major histocompatibility complex) class II molecules [73]. MHC molecules are classified into class I, II, III groups and are different in humans and mice called HLA and H-2, respectively [74]. MHC class I-restricted epitopes of influenza viruses are

better characterized than MHC class II-restricted epitopes of influenza viruses in murine models [75].

According to most of published literatures regarding CD4 T cell specific epitopes of influenza viruses, epitopes with high frequencies were derived from HA and NP [76]. Based on different murine models and virus isolates, the source and distribution of CD4 T cell epitopes would vary. In C57BL/6 mice after infection of influenza A/HK-x31, a large number of MHC class II-restricted epitopes (around 20-30) were unevenly distributed within limited proteins, with the majority deriving from NP and HA [75]. However, in BALB/c mice, multiple epitopes were also identified in NA of x31 viruses [75].

According to the study involving HLA-DR1 transgenic (DR1 Tg) mice and a human influenza isolate A/New Caledonia/20/99 (NC), the repertoire of HA-specific CD4 T cells after primary NC infection was very diverse [77]; More than 30 epitopes were identified within the entire HA protein, including epitopes genetically conserved across H1, H2, and H5 influenza viruses [77]. Besides HA, CD4 T cell specific epitopes were also identified in NA, NP and NS [77].

Different hosts express distinct MHC class II molecules, resulting in different repertoires of CD4 T cells. The immune response in DR1 Tg mice containing a human MHC class II molecule may accurately reflect the immune response in humans after natural influenza virus infection. In addition to the CD4 T cell response, the B cell response is another important component of the adaptive immune response against influenza viruses. However, the B cell response in DR1 Tg mice after primary NC infection has not been investigated. In this study, our goals were to characterize B cell responses after NC infection in DR1 Tg mice and

establish the correlation of B cell responses with CD4 T cell responses in the same mouse model system.

CHAPTER 2

MATERIALS AND METHODS

I. Mice

HLA-DR1 transgenic mice were got from Dr. Zaller (Merck) through Taconic laboratories and were housed and propagated under specific pathogen-free conditions at the animal center of the University of Tennessee. Mice were immunized at 2-3 months of age and were thereafter kept in BSL-2 containment.

C57BL/10J mice purchased from The Jackson Laboratory were housed under specific pathogen-free conditions until immunization and thereafter in BSL-2 containment. Female mice were used in all experiments and were infected at 8-12 weeks of age.

The Animal Care and Use Committee of the University of Tennessee approved all animal procedures.

II. Viruses

Influenza virus A/New Caledonia/20/99 (NC) grown and titrated in the allantoic cavity of embryonated hen's eggs was obtained from Dr. Richard Webby (St. Jude Children's Research Hospital, Memphis, TN). Influenza virus A/Puerto Rico/8/1934 (PR8) was grown and titrated in the allantoic cavity of embryonated hen's eggs.

Clone G2.4 of MHV-68 was originally obtained from Dr. A. A. Nash (Edinburgh, U.K.), and virus stocks were grown in owl monkey kidney cells and titrated on NIH-3T3 cells.

Viruses were inactivated by treatment with ß-propiolactone. Viral protein concentrations were measured using the Bio-Rad protein

assay kit (Bio-Rad, Hercules, CA). All virus preparations were stored at -80 °C

III. Immunization of mice

Mice were anesthetized with Avertin (2,2,2-tribromoethanol) given intraperitoneally before all immunizations.

For intranasal (i.n.) infection, mice were infected with 20,000-40,000 50% egg infectious doses (EID_{50}) of NC, or 25 EID_{50} of PR8, or 10^4 PFU of MHV-68 (30 µl in PBS).

For intramuscular (i.m.) immunization, a total dose of 20 µg of inactivated NC was given in two injections, each of 10 µg (50 µl in PBS), into the tibialis anterior muscle of each leg. A plastic sleeve over the needle was used to control the depth of injections.

IV. Tissue dissection and treatment

Anesthetized mice were exsanguinated via the retro-orbital plexus before organs were collected. Organs were processed to generate single-cell suspensions in IMDM media (Invitrogen, Carlsbad, CA) containing *L*- glutamine (2 mM), sodium pyruvate (1 mM), penicillin (100 IU/ml), streptomycin (100 µg/ml), gentamicin (10 µg/ml), and 5 $\times$ 10^{-5} M ß-mercaptoethanol (designated B cell medium), and supplemented with 10% FBS. Lymph nodes (CLN, MLN, PLN, IliLN, IngLN) and spleens were collected and gently disrupted between frosted ends of microscope slides. Bone marrow (BM) cell suspensions were obtained by flushing femurs and tibiae. Red

blood cells (RBCs) were removed from spleen and BM preparations by ammonium chloride lysis. Lungs were perfused with PBS prior to collection, and then were finely minced and incubated for 1 hour at 37 °C in BCM containing 10% FBS and 4 mg/ml collagenase type II (Worthington, Lakewood, NJ). Cells pelleted from the lung digest were resuspended in 40% isotonic Percoll and layered over 75% isotonic Percoll. After centrifugation at 600 × g for 20 min at 25 °C, cells at the interface were collected and washed. Lungs to be titrated for infectious viruses were homogenized in 1 ml HBSs containing antibiotics and 0.1% BSA. Homogenates were clarified by centrifugation, and supernatants were collected and stored at -80°C. Sera were collected from clotted blood and stored at -80 °C for antibody analysis.

V. ELISPOT assay

A preparation of concentrated viral particles was disrupted for 10 min at room temperature in a 1 in 10 dilution of disruption buffer (0.5% Triton X-100, 0.6 M KCl, and 0.05 M Tris-HCl, pH7.5) in PBS, further diluted in PBS, and plated at 1 μg/well in nitrocellulose-bottomed 96-well MultiScreen HA filtration plates (Millipore, Bedford, MA). After overnight incubation at 4°C, plates were washed with PBS, and then were blocked with BCM containing 10% FBS for 1 hour. Plates were emptied by flicking, and were washed with PBS. Single-cell suspensions were then added to plates in a volume of 100 μl/well. After incubation for 3-4 hours at 37°C in a humidified atmosphere containing 5% CO_2, plates were thoroughly washed with PBS alone and PBS containing 0.1% Tween 20. Alkaline Phosphatase-conjugated Goat Anti-Mouse IgGs, IgM, IgA (Southern Biotechnology, Birmingham, AL) diluted to 2 μg/ml in

PBS containing 5% BSA were added to plates in a volume of 100 µl/well, and plates were then incubated overnight at 4°C. Plates were washed thoroughly with PBS alone and PBS containing 0.1% Tween 20, including washing the underside of the nitrocellulose filter. Spots were developed at room temperature by adding 100 µl/well of 1 mg/ml of 5-bromo-4-chloro-3-indolylphosphate (Sigma, St. Louis, MO) in diethanolamine buffer (10% diethanolamine, 0.1 M NaCl, 5 mM $MgCl_2$, and 0.1 M Tris-HCl, pH 9.5). After optimal spots development, plates were washed with PBS and dried at room temperature. Spots representing individual antibody secreting cell (ASC) were counted using an Olympus SZX9 stereozoom microscope.

VI. ELISA

A preparation of concentrated viral particles was disrupted for 10 min at room temperature in a 1 in 10 dilution of disruption buffer (0.5% Triton X-100, 0.6 M KCl, and 0.05 M Tris-HCl, pH 7.5) in PBS, further diluted in PBS, and plated at 0.5 µg/well in 96-well flat bottom immuno plates (Nalge Nunc International, Rochester, NY) in a volume of 50 µl/well. After overnight incubation at 4°C, plates were washed with PBS containing 0.05% Tween 20, and were blocked with PBS containing 3% BSA for at least 90 min in a volume of 150 µl/well at room temperature. Plates were emptied by flicking, and were washed with PBS containing 0.05% Tween 20. Serum samples were serially 3-fold diluted in PBS containing 0.5% BSA and 0.05% Tween 20, and were added to plates in a volume of 50 µl/well. Plates were incubated for 3-4 hours at room temperature or overnight at 4°C, and then were washed with PBS containing 0.05% Tween 20. Alkaline Phosphatase-conjugated

Goat Anti-Mouse Abs with specificities for IgGs, IgA, IgM or Ig (H+L) (Southern Biotechnology, Birmingham, AL) diluted in PBS containing 1% BSA were added in a volume of 100 µl/well, and plates were incubated for 2-4 hours at room temperature or overnight at 4°C. After plates were washed with PBS containing 0.05% Tween 20, color was developed by adding 5 mg/15ml of p-nitrophenyl phosphate substrate (Sigma, St. Louis, MO) in diethanolamine buffer (10% diethanolamine, 0.1 M NaCl, 5 mM $MgCl_2$, and 0.1 M Tris-HCl, pH 9.5) in a volume of 100 µl/well at room temperature for 20-30 min. Absorbance was measured at 405 nm in the Synergy 2 multi-Detection Microplate Reader using Gen5 software (Biotek). Titers of virus-specific Abs were determined as the reciprocal of the highest dilution giving an absorbance value larger than 0.1 and at least two-fold higher than the absorbance of simultaneously titrated naïve samples.

VII. Virus titration

Viral titers in lung homogenates were determined by 50% tissue culture infection dose ($TCID_{50}$) using Madin-Darby Canine Kidney (MDCK) cells grown in MEM medium (Invitrogen, Carlsbad, CA) containing *L*- glutamine (2 mM), penicillin (100 IU/ml), streptomycin (100 µg/ml), gentamicin (10 µg/ml), and supplemented with 5% FBS. Confluent cell monolayer in a 96-well tissue culture plate was washed twice with FBS-free MEM medium containing 0.3% BSA immediately before the transfer of viral inocula. Serial 10-fold dilutions of lung homogenates were prepared on a 96-well round bottom polypropylene plate (Corning Incorporated, Corning, NY). Add 225 µl of MEM containing *L*- glutamine (2 mM), penicillin (100 IU/ml), streptomycin (100 µg/ml), gentamicin (10 µg/ml), 0.3% BSA

and 2 μg/ml *L*-(tosylamido-2-phenyl) ethyl chloromethylketone (TPCK) -treated Trypsin (Worthington, Lakewood, NJ) (designated VGM) to every well. Add 25 μl of lung homogenates to the first well of each row. Mix and transfer 25 μl to successive wells to generate 10-fold dilutions. Transfer 200 μl of lung homogenate dilutions to corresponding wells of the washed MDCK cells plate. After 2-3 days incubation at 37°C in a humidified atmosphere containing 5% CO_2, observe the plate under an inverted microscope for viral CPE, and draw 50 μl/well of supernatants to perform HA assay. Calculate the $TCID_{50}$ by the Reed-Muench method.

VIII. Hemagglutination assay (HA)

Orient a 96-well round bottom polystyrene assay plate (Corning Incorporated, Corning, NY) so that samples will be diluted 12 wells across. Number the row on each plate to identify different samples. Add 50 μl PBS to every well on the plate. Add virus suspensions or cell culture supernatants to the first well in each row in a volume of 50 μl. Note that this will result in a 1:2 dilution of the test sample in the first well. A positive control and a negative control (such as PBS only) must be included. Mix the content of the first well by pipetting up and down 10 times and transfer 50 μl to successive wells to make 2-fold dilutions of the sample across the entire row. Discard the final 50 μl after the last row. At this point every well should have a volume of 50 μl. Add 50 μl of 0.5% chicken red blood cells (RBCs) suspension (Fitzgerald, Concord, MA) to every well. Mix the plate by using a mechanical vibrator or by taping the plate gently. Incubate the plate at room temperature for an appropriate time (30-60 min) by checking negative control wells for complete settling of RBCs.

Results of the HA assay should be interpreted when RBCs in negative control wells had settled down to form solid buttons at the bottom of wells (hemagglutination-negative). When the plate was tilted at approximate 45-degree, RBCs in negative control wells would stream down in a “tear-drop” fashion. Samples that were hemagglutination-negative should also form solid buttons at the bottom of wells and slide down at the same rate as negative controls. Samples showing complete hemagglutination in one or more wells were considered hemagglutination-positive. Incomplete hemagglutination was observed as buttons that did not slide, had fuzzy margins, or formed a doughnut-shaped ring at the bottom of wells. The endpoint of a sample was the highest dilution causing complete hemagglutination. The endpoint dilution was considered containing one hemagglutination unit (HAU), and the number of HAUs/50 μl was the reciprocal of the highest dilution.

IX. Hemagglutination inhibition assay (HAI)

a. Treatment of sera

Sera against influenza viruses prepared in most animals (ferret, rabbit, mouse) must be treated with receptor destroying enzyme (RDE) to eliminate nonspecific hemagglutination inhibitors. RDE (II) “SEIKEN” (Denka Seiken CO. LTD, Tokyo, Japan) was completely dissolved in 20 ml of sterile physiological saline, 0.85% NaCl. This solution should be used immediately or be aliquot and stored at - 20°C or less. Under sterile condition add 3 vols of RDE to 1 vol of sera (such as 90 μl RDE + 30 μl sera), and mix

thoroughly. Heat the mixture in a 37°C waterbath for 18-20 hours to allow the reaction to occur. Then heat the mixture in a 56°C waterbath for 30-60 min to inactivate remaining RDE. Allow the mixture to cool down to room temperature. Add 6 vols of sterile physiological saline, 0.85% NaCl (such as 180 µl). The final dilution of the sera was 1:10.

b. HA titration of the control antigen

The control antigen was titrated by following the procedure of hemagglutination assay described above. The endpoint of a sample was the highest dilution causing complete hemagglutination. The endpoint dilution was considered containing one hemagglutination unit (HAU), and the number of HAUs/50 µl was the reciprocal of the highest dilution. Calculate the HAUs/50 µl of the control antigen.

c. Preparation of standardized antigens for HAI and “Back titration”

Standardized antigens used for HAI should have 4 HAUs/25 µl or 8 HAUs/50 µl. Calculate the antigen dilution by dividing the HAUs/50 µl of the control antigen by 8 in order to get 8 HAUs/50 µl of standardized antigens. Make the dilution in an appropriate volume.

The “back titration” was performed by doing HA assay to verify the 8 HAUs/50 µl of standardized antigens. Add 50 µl PBS to well #1-6 on a 96-well microtiter plate. Add 50 µl standardized antigens (8 HAUs/50 µl) to well #1. Mix and

transfer 50 µl to successive wells to make serial 2-fold dilutions until well #6. Discard the final 50 µl. Each well should contain 50 µl after this step. Add 50 µl 0.5% RBCs to each well. Mix the plate by using a mechanical vibrator or taping gently. Incubate the plate at room temperature for 30-60 min to allow RBCs to settle down at the bottom of wells. The first three wells should be hemagglutination-positive. Store standardized antigens at 4°C and use within the same day.

d. Hemagglutination inhibition (HAI)

Orient a 96-well round bottom polystyrene assay plate (Corning Incorporated, Corning, NY) so that samples will be diluted 8 wells across. Add 25 µl PBS to wells of row B through G (B1-G12). Add 50 µl RDE-treated samples (1:10) to wells of row A (A1-A12) and add 25 µl the same RDE-treated samples (1:10) to wells of row H (H1-H12) as well. Prepare serial 2-fold dilutions of treated samples by transferring 25 µl from row A to successive wells until row G. Discard the final 25 µl after row G. Add 25 µl standardized antigens to wells of row A through G (A1-G12). Add 25 µl PBS instead of standardized antigens to wells of row H (H1-H12). Mix the plate by using a mechanical vibrator or taping gently. Incubate the plate at room temperature for 1 hour. Add 50 µl 0.5% RBCs to every well, and mix as before. Incubate the plate at room temperature for an appropriate time for RBCs settling. The HAI titer was the reciprocal of the highest dilution of the sample that completely inhibited

hemagglutination of standardized antigens. Record HAI titers of samples.

X. Neutralization assay

a. Preparation of test samples

Sera samples were treated with RDE as described above in HAI assay. Orient a 96-well round bottom polypropylene assay plate (Corning Incorporated, Corning, NY) so that samples would be diluted 12 wells across. Add 60 µl VGM to wells of column 2 through 12. Add 120 µl the RDE-treated sample (1:10) to the first well of each row. Prepare serial 2-fold dilutions by transferring 60 µl from the first well to successive wells until column 12 and discard the final 60 µl. Each well should contain 60 µl sample dilutions after this step.

b. Addition of standardized viruses and “back titration”

Standardized viruses contain 50 $TCID_{50}$/50 µl in VGM. Add 60 µl standardized viruses to each well except cell control wells. Add 60 µl VGM instead of standardized viruses to cell control wells.

Set up “back-titration” as follows on a separate 96-well round bottom polypropylene assay plate. This required quadplications of ½ lg dilutions of standardized viruses. Add 120 µl VGM to wells of column 2 through 8, and then add 175 µl standardized viruses (50 $TCID_{50}$/50 µl) to the first column.

Generate ½ lg dilutions by transferring 55 µl from the first well to successive wells. Discard the final 55 µl.

Plates containing sample/virus mixture, virus back-titration and cell controls were gently agitated and incubated at 37°C in a humidified atmosphere containing 5% CO_2 for 2 hours.

c. Inoculation of MDCKs and HA assay

During the final 15-30 min of the incubation period, wash confluent MDCK monolayers in 96-well cell culture plates with 200 µl/well MEM containing 0.3% BSA twice. After the completion of 2 hours incubation period of sample/virus mixtures, empty the last wash of MDCK monolayers, and transfer 100 µl/well sample/virus mixtures to corresponding wells in MDCK cell plates. Change tips for each transfer. Add 100 µl VGM to each well to bring the final volume in MDCK plates to 200 µl/well. Incubate MDCK plates at 37°C in a humidified atmosphere containing 5% CO_2 for 2-3 days. Then draw 50 µl/well supernatants to perform HA assay. The neutralizing Abs titer of the sample was the reciprocal of the highest dilution of the sample that completely prevented virus infection of MDCK cells.

XI. Cell surface staining and flow cytometry

Single-cell suspensions from lymph nodes (CLN, MLN) and spleens were stained as follows. Add 1×10^6 cells to designated wells of a 96-well round bottom plate. Centrifuge the plate at 1500 rpm for 5 min at room temperature. Flick off the supernatant and vortex the

plate to resuspend cells. Block cells with 100 µl/well Fc blocking antibody or normal naïve mice serum diluted 1/200 or 1/100, respectively, in PBS containing 2% FBS and 0.05% sodium azide (FACS buffer). Cells were resuspended thoroughly and incubated on ice for 30 min. Centrifuge the plate as before, flick off the supernatant and vortex the plate to resuspend cells. Dilute primary antibodies 1/200 in FACS buffer, and add to appropriate wells in a volume of 100 µl/well and mix thoroughly. For the unstained well, add 100 µl of PBS instead of primary antibody dilution. Wrap the plate with foil and incubate the plate on ice for 30 min. Centrifuge the plate as before, flick off the supernatant and resuspend cells with 100 µl/well FACS buffer. Transfer cell suspensions to 5 ml polystyrene round bottom tubes (Becton Dickinson, Franklin Lakes, NJ). Add 600 µl of FACS buffer to each tube. Keep samples on ice and covered until ready to run using FACScan and Cellquest software. For the analysis of germinal center B cell differentiation, cells were stained with PE-conjugated anti-Fas, PerCP-conjugated anti-B220 (BD Biosciences), and FITC-conjugated-Peanut agglutinin (PNA) (Vector Laboratories. Inc., Burlingame, CA).

XII. Statistics

Statistical comparisons of mean values were performed using the unpaired T test for unpaired samples. Values of $p < 0.05$ were considered statistically significant.

CHAPTER 3

RESULTS

I. B cell responses in HLA-DR1 transgenic mice and C57BL/10J mice after intranasal infection of influenza virus NC

a. Kinetic analyses of influenza-specific Abs responses to intranasal administration of influenza virus NC

To explore influenza-specific ASCs responses in DR1 Tg mice, naïve mice were infected with NC intranasally, and draining lymph nodes, spleens, BMs and lungs were collected at different time intervals post-infection. B10 mice were included to compare with DR1 Tg mice in this experiment. The kinetics of NC-specific ASCs responses in CLNs, MLNs, spleens, BMs and lungs were showed in Fig. 1. On day 8 after virus infection, the virus-specific response in the MLN of B10 mice slightly preceded responses in the MLN of DR1 Tg mice, suggesting in DR1 Tg mice the humoral response was delayed by some factors. In DR1 Tg mice, peak numbers of virus-specific ASCs showed up in the CLN, MLN, and spleen subsequent to 2 weeks after infection and progressively decreased from 2 to 3 weeks after infection. The virus-specific ASCs response in DR1 Tg mice was characterized by predominant IgG1 isotype switching, which was not observed in B10 mice. Virus-specific ASCs appeared in the BM and lung between 2 and 3 weeks after influenza infection, and IgG1 was the predominant switched isotype in DR1 Tg mice which was consistent with ASCs isotype profiles in draining LNs and spleens.

Levels of virus-specific Abs in sera closely reflected the single cell analysis of the B cell response (Fig. 2). In DR1 Tg mice, the titer of IgG1 was higher than other isotypes, and titers of all isotypes were lower on day 8 than that of B10 mice. Regardless of

different isotypes, the titer of virus-specific Ig in sera was lower in DR1 Tg mice compared to B10 mice on days 8 and 10 after infection, reflecting the delayed B cell response in DR1 Tg mice (Fig. 3, A). The neutralization assay was conducted to measure the titer of neutralizing Abs. DR1 Tg mice showed significantly higher neutralizing Abs titers than B10 mice ($p < 0.05$) on day 14 after infection. Also DR1 Tg mice demonstrated stronger hemagglutination inhibition activity than B10 mice on day 14 after infection ($p < 0.05$). Taken together, the acute immune response following i.n. NC infection was skewed towards the IgG1/Th2 bias with higher neutralizing Abs titers and HAI titers in DR1 Tg mice.

The kinetics of the viral growth was determined by $TCID_{50}$ using lung homogenates of infected mice (Fig. 4). At early time points after infection there was no difference between DR1 Tg mice and B10 mice. However, on day 10 viruses were still detectable in DR1 Tg mice but became cleared in B10 mice, suggesting that virus clearance was slower in DR1 Tg mice compared to B10 mice.

b. Germinal center formation and the comparison of influenza-specific and non-specific ASCs responses after intranasal administration of influenza virus NC

Based on the intriguing observation of the IgG1/Th2 bias and higher neutralizing Abs titers in DR1 Tg mice, we analyzed the GC reaction in MLNs after i.n. NC infection in DR1 Tg mice and B10 mice. We identified by flow cytometry a distinct population of germinal center B cells, stained with anti-B220 and anti-Fas monoclonal antibodies and the peanut agglutinin (PNA), in both

DR1 Tg mice and B10 mice. In DR1 Tg mice, percentages of germinal center B cells ($B220^{+}PNA^{hi}Fas^{hi}$) in MLNs were similar with B10 mice on days 8,10, and 14, but higher than B10 mice on day 21 (Fig. 5, A). When we compared frequencies of germinal center B cells per lymph node, there was no difference between two groups (Fig. 5, B). But if the frequency of germinal center B cells were calculated per 10^6 lymphocytes or per 10^5 B-lymphocytes, significant difference was showed on day 21 after infection (Fig. 5, C-D).

Previous studies suggested that strong early polyclonal B cell activation competed with virus-specific B cell activation and the formation of neutralizing Abs [78]. Virus-specific and non-virus-specific ASCs frequencies in MLNs were determined after i.n. NC infection in DR1 Tg mice and B10 mice. Since the immune response was delayed in DR1 Tg mice, the non-specific response also started later on day 10 post infection, with IgG1 predominating and minimal other isotypes (Fig. 6). The non-specific ASC response in DR1 Tg mice was weaker compared with the massive non-specific B cell response in B10 mice at early stage. In B10 mice, total ASCs numbers peaked on day 8 post-infection and decreased gradually on day 10 and 14. And isotype profiles of virus-specific and total ASCs responses were similar showing switched IgG2c bias in B10 mice (Fig. 6).

II. B cell responses in HLA-DR1 transgenic mice and C57BL/10J mice after intramuscular immunization of influenza virus NC

Puzzled by the IgG1/Th2 bias in DR1 Tg mice after i.n. NC infection, we wondered whether it was a characteristic of immune responses of DR1 Tg mice. We immunized DR1 Tg mice and B10 mice with inactivated NC intramuscularly and collected draining LNs and spleens to determine virus-specific ASCs frequencies on days 8 and 11 post immunization. Isotype profiles were strikingly similar between DR1 Tg mice and B10 mice, characterized by IgM predominance in the IngLN, IliLN, and spleen on day 8 and predominant IgG2c isotype switching on day 11 (Fig. 7). In DR1 Tg mice the observed predominance of switched IgG1 after i.n. NC infection was replaced by the IgG2c bias after i.m. administration.

III. B cell responses in HLA-DR1 transgenic mice and C57BL/10J mice after intranasal infection of influenza virus PR8

Since the i.m. vaccination induced a different isotype profile of B cell responses in DR1 Tg mice, we tested a different influenza virus isolate to see whether the immune response profile could be different. In this experiment, mice were infected with PR8 (H1N1) intranasally. In contrast to i.n. NC infection, PR8 infection induced earlier and stronger B cell responses in DR1 Tg mice, with massive IgM production starting on day 6 and peaking on day 8 (~ 20-fold of that of NC infection). Then the early peak of virus-specific IgM ASCs gave way to increased numbers of cells producing IgG isotypes, particularly IgG3 (Fig. 8, B). Compared with i.n. NC infection, PR8 infection obviously did not modify the isotype profile of B cell responses in B10 mice (Fig. 8, A), showing the same IgG2c predominance. Serum levels of virus-specific Abs also reflected the single cell analysis of B cell responses (Fig. 9).

And DR1 Tg mice showed higher neutralizing Abs titers than B10 mice on day 10 after PR8 infection (Fig. 10, A).

Influenza virus PR8 is a mouse-adapted strain, while NC has not been adapted to grow in mice. So we wondered whether the virus replication was different between the two strains. The viral load in the lung after i.n. PR8 infection was measured by $TCID_{50}$ using lung homogenates. There was no significant difference on viral titers between DR1 Tg mice and B10 mice on days 6, 8, and 10 after PR8 infection (Fig. 10, B). And when we compared the viral titer between i.n. NC infection and i.n. PR8 infection on day 8 in DR1 Tg mice and B10 mice, respectively, no difference was observed (data not shown). However, because the infection dose of NC was ~ 400 fold of PR8, it was obvious that PR8 replicated better than NC in mice. Therefore, although viral titers in the lung were similar on day 8 after NC and PR8 infection, the better PR8 virus replication in the lung may induce different cytokines production and resulted in different B cell immune responses.

IV. B cell responses in HLA-DR1 transgenic mice and C57BL/10J mice co-infected with NC and MHV-68 viruses intranasally

Previous studies showed i.n. MHV-68 infection mainly induced the IgG2a/IgG2b production with a low level of IgG1 production [79]. So we were interested in whether the Th2 biased B cell response in DR1 Tg mice following i.n. NC infection could be altered by a co-infection with MHV-68, which is a Th1 biased virus. In this experiment, co-infected mice were sampled on days 8 and 10 after co-infection and MLNs were collected to conduct ELISPOT assay

to enumerate NC-specific and MHV-68-specific ASCs, respectively. In both DR1 Tg mice and B10 mice, MHV-68-specific IgM ASCs peaked on day 8 and was followed by increased IgGs isotypes switching, especially the IgG2c (Fig. 11, B and D). The kinetics and isotype profiles of NC-specific B cell responses were similar in co-infected DR1 Tg mice and B10 mice, demonstrating a IgG2c biased immune response. However, the co-infection induced different NC-specific ASCs responses in DR1 Tg mice compared with i.n. NC infection. The NC-specific ASCs response was changed to Th1 bias in co-infected DR1 Tg mice, with IgG2c predominating (Fig. 11, A and C), meanwhile the i.n. NC infected DR1 Tg mice still displayed Th2 biased responses with IgG1 predominance. Overall, the co-infection of MHV-68 and NC viruses successfully switched the NC-specific humoral response from a Th2 bias to a Th1 bias in DR1 Tg mice. The mechanism behind this observation was still unclear.

The dispersion of different isotypes of circulating NC-specific Abs in sera also reflected the ASCs response. Isotype profiles were similar after co-infection between DR1 Tg mice and B10 mice, showing higher NC-specific IgG2c production than IgG1 (Fig. 12, A-D). But neutralizing Abs titers were below the limit of measurement in both groups. Since the NC-specific immune response was changed by co-infection with MHV-68 virus compared with i.n. NC infection, we wanted to know whether the virus replication in the lung was also changed. By comparing virus titers between NC-only infection and co-infection groups on day 8, no significant difference was observed.

Figure legend

Fig. 1 The primary influenza-specific ASCs response to intranasal administration of NC in DR1 Tg mice and B10 mice. The kinetics of virus-specific ASC responses in the CLN (A), MLN (B), spleen (C), lung (D) and BM (E) were determined in mice infected with NC intranasally. The ELISPOT assay was used to enumerate virus-specific ASCs in single cell suspensions from individual mouse. Results were expressed as the number of ASCs/10^5 nucleated cells or the number of ASCs/$5x10^5$ nucleated cells. CLN, cervical lymph node; MLN, mediastinal lymph node; BM, bone marrow. Data were mean + SE (n > 3).

Fig. 2 The influenza-specific Abs level in serum after intranasal administration of NC in DR1 Tg mice and B10 mice. The kinetics of virus-specific Abs titers of different isotypes, IgG1 (A), IgG2b (B), IgG2c (C), IgG3 (D), IgM (E), IgA (F), were measured by ELISA. Results were determined by endpoint titration and did not necessarily reflect the relative amount of each isotype. Data were mean + SE (n > 3).

Fig. 3 The influenza-specific immunoglobulin level and neutralizing Abs titers and hemagglutination inhibition titers in serum after intranasal administration of NC in DR1 Tg mice and B10 mice. (A) The kinetics of virus-specific Ig was measured by ELISA and results were determined by endpoint titration. (B) Neutralizing Abs titers in serum were measured by neutralization assay. Results were expressed as the reciprocal of the highest serum dilution completely preventing virus infection of MDCK cells. (C) HAI titers in serum were measured by hemagglutination inhibition assay and results were expressed as the reciprocal of the highest serum dilution completely inhibiting hemagglutination activity of standardized viruses.

Fig. 4 Virus replication in the lung after intranasal infection of NC in DR1 Tg mice and B10 mice. Lungs of infected mice were collected at different time intervals post-infection. Lung homogenates were used to perform $TCID_{50}$. Viral titers were determined by endpoint dilution that infected 50% MDCK cells. Results were expressed as $log_{10}TCID_{50}$ / 0.2 ml lung homogenates. Data were mean + SE (n > 3).

Fig. 5 Germinal center formation in the MLN of DR1 Tg mice and B10 mice after i.n. NC infection. Lymphocytes were isolated and analyzed on days 8, 10, 14 and 21 after infection. (A) Flow cytometry of germinal center B cells in the MLN. Gated $B220^+$ B cells were shown. $PNA^{hi}Fas^{hi}$ germinal center B cells were boxed, with the percentage of $B220^+$ B cells indicated. (B) The number of germinal center B cells ($B220^+PNA^{hi}Fas^{hi}$) per MLN. (C-D) Frequencies of germinal center B cells expressed as the number of $B220^+PNA^{hi}Fas^{hi}$ per 10^6 lymphocytes or 10^5 $B220^+$ cells, respectively. MLN, mediastinal lymph node. Data were mean + SE (n > 3).

Fig. 6 Comparison of influenza-specific and non-specific ASCs responses in the MLN of DR1 Tg mice and B10 mice following intranasal infection of NC. MLNs were collected from infected mice on days 10 (A) and 14 (B) after infection. The ELISPOT assay was used to enumerate ASCs in single cell suspensions from individual mouse. Purified NC viruses and goat anti-mouse Abs were used to coat ELISPOT plates, respectively. Results were expressed as the number of ASCs/10^5 nucleated cells. MLN, mediastinal lymph node.

Fig. 7 The primary influenza-specific ASCs response to intramuscular administration of inactivated NC in DR1 Tg mice and B10 mice. Mice were sampled at days 8 and 10 after i.m vaccination with inactivated NC.

IngLNs (A), IliLNs (B), and spleens (C) were collected on day 8 and PLNs (D), IliLNs (E) and spleens (F) were collected on day 10. The ELISPOT assay was used to enumerate virus-specific ASCs in single cell suspensions from individual mouse. Results were expressed as the number of ASCs/$5x10^5$ nucleated cells. IngLN, inguinal lymph node; IliLN, iliac lymph node; PLN, popliteal lymph node. Data were mean + SE (n > 3).

Fig. 8 The influenza-specific ASCs response to intranasal administration of influenza virus PR8 in DR1 Tg mice and B10 mice. MLNs of B10 mice (A) and DR1 Tg mice (B) were collected and processed into single cell suspensions on days 6, 8 and 10 after i.m. immunization. The ELISPOT assay was used to enumerate PR8-specific ASCs from individual mouse. Results were expressed as the number of ASC/10^5 nucleated cells. MLN, mediastinal lymph node. Data were mean + SE (n > 3).

Fig. 9 Influenza-specific Abs levels in serum after intranasal infection of PR8 in DR1 Tg mice and B10 mice. The kinetics of virus-specific Abs titers of different isotypes, IgG1 (A), IgG2b (B), IgG2c (C), IgG3 (D), IgM (E), and IgA (F), were determined by ELISA. Results were determined by endpoint titration and did not necessarily reflect the relative amount of each isotype. Data were mean + SE (n > 3).

Fig. 10 Neutralizing Abs titers in serum and viral growth in the lung after intranasal infection of PR8 in DR1 Tg mice and B10 mice. (A) Neutralizing Abs titers in serum were determined by neutralization assay. Results were expressed as the reciprocal of the highest dilution of the serum completely preventing virus infection of MDCK cells. (B) Lung homogenates of infected mice were used to perform $TCID_{50}$ to measure the virus growth in lungs. Viral titers were determined by endpoint dilution that infected 50%

MDCK cells. Results were expressed as $log_{10}TCID_{50}$ /0.2 ml lung homogenates.

Fig. 11 Influenza-specific ASCs responses in mice co-infected with NC and MHV-68 viruses. DR1 Tg mice and B10 mice were intranasally infected by NC and MHV-68 viruses. MLNs were collected on days 8 (A-B) and 10 (C-D) post-infection. The ELISPOT assay was used to enumerate virus-specific ASCs from individual mouse. Purified NC viruses and purified MHV-68 viruses were used to coat ELISPOT plates to measure NC-specific ASCs (A, C) and MHV-68-specific ASCs (B, D), respectively. Results were expressed as the number of ASCs/10^5 nucleated cells. MLN, mediastinal lymph node.

Fig. 12 Influenza-specific Abs levels in serum of mice co-infected with NC and MHV-68 viruses. Titers of different NC-specific isotypes (A-D) and NC-specific immunoglobulin (E) were determined by ELISA. Results were determined by endpoint titration and did not necessarily reflect the relative amount of each isotype. (F) Comparison of viral titers in lungs between NC-only and co-infected mice on day 8. Virus titers were determined by endpoint dilution that infected 50% MDCK cells. Results were expressed as $log_{10}TCID_{50}$ / 0.2 ml lung homogenates.

CHAPTER 4

DISCUSSION

The transgenic mouse model system used in this study contains a human MHC class II molecule HLA-DR1 [80-82] and provides a useful model for evaluating the diversity and specificity of CD4 T cell responses that may develop in humans following influenza virus infection or vaccination [77, 83]. The influenza virus A/New Caledonia/20/99 (NC) used in the study is not a mouse-adapted isolate and has been circulating in the North American human populations for more than 10 years [84]. The influenza-specific B cell response to intranasal administration (i.n.) of NC was analyzed in HLA-DR1 transgenic mice (DR1 Tg) and in the genetically matched *H-2*^{b} strain C57BL/10J (B10). The B cell ELISPOT assay was used to characterize the production of virus-specific ASCs at the single cell level. In B10 mice, the B cell response in draining LNs was typical of previously described B cell responses to a variety of mouse-adapted influenza viruses, characterized by a Th1 bias, as indicated by a stronger IgG2c production. In contrast, the B cell response in DR1 Tg mice followed delayed kinetics and was strongly skewed to a Th2 bias, as indicated by a stronger IgG1 production. This phenomenon was observed in draining LNs and spleens. Another interesting feature of the B cell response to NC infection in DR1 Tg mice was that there were higher neutralizing Abs titers and hemagglutination inhibition (HAI) titers on day 14 after virus infection compared with B10 mice.

However, the IgG1/Th2 bias was not a characteristic of all B cell responses in DR1 Tg mice. After intramuscular vaccination of inactivated NC, the virus-specific B cell response displayed a strong IgG2c/Th1 bias instead of the IgG1 skewing in draining LNs and spleens. This feature was also evident when PR8 (H1N1 isolate) was given intranasally. The PR8-specific B cell response after intranasal infection demonstrated a totally different isotype profile, demonstrating a massive PR8-specific IgM/IgG3

production. The virus-specific IgG1 skewing which was evident after i.n. NC infection in DR1 Tg mice was also abolished. Based on these observations, we concluded that the unusual IgG1/Th2 bias was restricted to the intranasal infection of NC in DR1 Tg mice.

Additional experiments were conducted to probe the mechanism behind the NC-specific IgG1/Th2 bias in DR1 Tg mice. Murine gammaherpesvirus 68 (MHV-68) is a member of the γ-herpesvirus family, that infects epithelial cells and mononuclear cells in the lower respiratory tract [85]. A previous study showed that MHV-68-specific B cell responses after i.n. infection were characterized by a predominant IgG2a/IgG2b ASCs production and a low level of IgG1 production [79]. Therefore, we speculated that the Th2 biased B cell response in DR1 Tg mice following i.n. NC infection could be altered by a co-infection with MHV-68, which is a Th1 biased virus. Our data demonstrated that in co-infected DR1 Tg mice, the IgG1 biased NC-specific B cell response in draining LNs was abolished. Instead, the isotype profile skewed towards the IgG2c/Th1 bias. Notably, the MHV-68-specific response did not change as a result of the co-infection. The mechanism underlying this observation was still not clear.

The current study raised several questions, such as what factors drove the antibody isotype switching to IgG1 in DR1 Tg mice after i.n. NC infection, and why the neutralizing Abs titer and the HAI titer were higher although the titer of virus-specific immunoglobulin in serum was lower in DR1 Tg mice compared to B10 mice. The B cell activation is dependent on help signals received from CD4 T cells, and the priming of CD4 T cells relies on antigen presentations by professional APCs, especially infected dendritic cells (DCs) [86-88]. We speculated that the antigen presentation process after influenza virus infection contributed to these observations in DR1 Tg mice. The high level synthesis of viral proteins within infected DCs

could override some factors that usually restrict the presentation of endogenous peptides by MHC class II molecules, resulting in broader diversity of CD4 T cell specific repertoire [77]. Also higher numbers of antigen-bearing DCs in lymph nodes after influenza virus infection can help diversify the CD4 T cell specific repertoire by reducing the competition for antigens [89]. After intranasal infection, NC can replicate better in infected epithelial cells and DCs; but after intramuscular vaccination, NC lose the access to replicate in these cells. Therefore, antigen presentations by DCs after i.n. and i.m. could be quite different, resulting in distinct CD4 T cells priming and the down-stream B cell activation. In vitro studies have indicated that the up-regulated expression of MHC class II molecules and co-stimulatory molecules, like CD40 and OX40L, on activated DCs mediated Th2 differentiation [90, 91]. Current studies focusing on the CD4 T cell specific repertoire after NC virus infection showed a much broader distribution of CD4 T cells specific epitopes in DR1 Tg mice, while previous studies identified restricted CD4 T cell specific repertoire in C57BL/6 mice [75, 77, 83]. The CD4 T cell specific repertoire in B10 after NC primary infection was revealed to be narrow and was limited to certain proteins.

Besides different diversities of the CD4 T cell repertoire between DR1 Tg mice and B10 mice, different specificities of CD4 T cells may also play an important role in the immune response. One hypothesis underlying the current project is that B cells display a limited subset of influenza-derived peptides specificities that are mainly restricted to antigens from HA, NA and M2. The specificity of CD4 T cells that help Ag-specific B cells to produce neutralizing antibodies in vivo after influenza infection is largely restricted to these peptides derived from HA, NA and M2, especially the HA [83]. The remaining CD4 T cells with specificities for internal viral antigens may be counterproductive to the protective immunity by

occupying needed “space” in the CD4 T cell memory compartment [83]. T cells and B cells with the same specificity can form long-lasting cognate interactions which ensure B cells get essential and enough help signals to undergo further differentiation, immunoglobulin isotype switching and affinity maturation [92, 93]. Studies done by our collaborating lab at the University of Rochester (Andrea Sant’s lab) demonstrated that the repertoire of HA-specific CD4 T cells after primary influenza infection in DR1 Tg mice was very broad, containing more than 30 different specificities within the entire HA [77]. However, in B10 mice, the majority of CD4 T cell-specific epitopes were derived from NP and NA [94]. Therefore, the diverse HA-specific CD4 T cells in DR1 Tg mice would be more effective in activating HA-specific B cells and facilitating the neutralizing Abs production. On the other hand, in B10 mice, NP-specific CD4 T cells would weaken the HA-specific B cell activation and the neutralizing Abs production.

Help signals from activated CD4 T cells to B cells and CD8 T cells are mainly mediated by different cytokines. Cytokines from Th1 cells, like IL-2 and IFN-γ, can activate CD8 T cells and facilitate isotype switching to IgG2a/IgG2c; cytokines from Th2 cells, such as IL-4 and IL-5, mainly provide help for B cells activation and help IgA, IgE, and IgG1 production [34]. Therefore, we speculated that different cytokines profiles induced by i.n. NC infection might contribute to the IgG1/Th2 bias observed in DR1 Tg mice. Results from Andrea’s lab showed that similar levels of IL-4, IL-2 and IFN-γ were present in DR1 Tg mice after i.n. NC infection, while very minimal IL-4 was detected in B10 mice (data not shown). The Th2 type cytokine IL-4 in DR1 Tg mice quite possibly contributed to the IgG1/Th2 bias, while the predominance of Th1 type cytokines in B10 mice enabled the B cell response to polarize towards a Th1 bias. In addition, Th1 type cytokines in B10 mice would effectively activate CD8 T cells, which might

explain the rapid virus clearance observed in B10 mice after i.n. NC infection. In the co-infection experiment, the production of IFN-γ and IL-6 induced by MHV-68 infection might contribute to the isotype switching to IgG2c in DR1 Tg mice.

In this study we also compared the virus-specific and non-specific B cell activation after NC infection between DR1 Tg mice and B10 mice. In B10 mice, the virus-specific B cell response in the MLN was accompanied by a strong non-specific ASCs production on days 8 and 10, displaying IgG2c predominance. Since the immune response was delayed during the early phase after NC infection in DR1 Tg mice, both the virus-specific and non-specific responses were weak on day 8. The increase of non-specific ASCs was not significant on days 10 and 14, except the non-specific IgG1 ASCs. Research showed that strong and even normal virus-specific CD4 T cell activation resulted in an increased early polyclonal B cell activation, which competed with the virus-specific B cell activation and the formation of neutralizing Abs [78]. Polyclonal B cell activation was reflected by non-specific antibodies production and required the involvement of activated B cells in germinal center processes [79]. We speculated that the strong early non-specific B cell activation in B10 mice inhibited the virus-specific B cell activation and maybe responsible for the lower neutralizing Abs titer. But it was still unclear about the source and the function of the massive non-specific IgG1 ASCs in DR1 Tg mice.

Since the germinal center (GC) is the main place supporting the somatic hypermutation, the affinity maturation, and the formation of memory B cells [68], we compared the GC reaction in MLNs after i.n. NC infection between DR1 Tg mice and B10 mice by staining lymphocytes with GC markers peanut agglutinin (PNA) and Fas (also known as CD95) [95, 96]. We calculated the total number of GC B cells per lymph node and

found no difference between two groups. We also calculated the GC B cell frequency per 10^6 lymphocytes, and there was no difference, except on day 21 after infection. However, there are alternative ways to examine the GC B cell response by using different GC markers combinations, such as $B220^+PNA^{hi}$, $B220^+GI7^{hi}$, $B220^+IgD^{lo}Fas^{hi}PNA^{hi}CD38^{int}$, or $B220^+PNA^{hi}GI7^{hi}Fas^{hi}$ [95-98]. When we compared the percent of $B220^+PNA^{hi}$ population, there seemed to be a higher percentage of these cells in DR1 Tg mice than B10 mice. At this stage, the GC reaction has not been fully characterized in DR1 Tg mice and B10 mice, and it is still largely unclear whether the GC reaction is related to different immune response patterns. More experiments are needed in this direction in order to clarify this issue.

In addition to GC B cells, there are two other important cell types that are also involved in the GC reaction, follicular DCs and follicular helper T cells [96, 99]. Both of them play crucial roles in the BCRs affinity selection in the GC. Follicular helper T cells are a subset of activated CD4 T cells and are characterized by high expression of CXCR5 and co-stimulatory molecules CD40L and ICOS [70]. Follicular helper T cells can secrete high level of IL-4 and shape the B cell response, especially the IgG1 isotype switching and affinity maturation [96]. It will be interesting to perform experiments that will compare follicular helper T cells frequencies between DR1 Tg mice and B10 mice. Understanding the mechanism underlying the unusual IgG1/Th2 bias in DR1 Tg mice after i.n. NC infection can provide useful insights into the regulation of immunoglobulin isotypes expression in DR1 Tg mice.

REFERENCES

1. Tamura, S. and T. Kurata, *Defense mechanisms against influenza virus infection in the respiratory tract mucosa.* Jpn J Infect Dis, 2004. **57**(6): p. 236-47.
2. Cox, N.J. and K. Subbarao, *Global epidemiology of influenza: past and present.* Annu Rev Med, 2000. **51**: p. 407-21.
3. Cox, R.J., K.A. Brokstad, and P. Ogra, *Influenza virus: immunity and vaccination strategies. Comparison of the immune response to inactivated and live, attenuated influenza vaccines.* Scand J Immunol, 2004. **59**(1): p. 1-15.
4. Fouchier, R.A., et al., *Characterization of a novel influenza A virus hemagglutinin subtype (H16) obtained from black-headed gulls.* J Virol, 2005. **79**(5): p. 2814-22.
5. Horimoto, T. and Y. Kawaoka, *Influenza: lessons from past pandemics, warnings from current incidents.* Nat Rev Microbiol, 2005. **3**(8): p. 591-600.
6. Webster, R.G., et al., *Evolution and ecology of influenza A viruses.* Microbiol Rev, 1992. **56**(1): p. 152-79.
7. Lewis, D.B., *Avian flu to human influenza.* Annu Rev Med, 2006. **57**: p. 139-54.
8. Steinhauer, D.A. and J.J. Skehel, *Genetics of influenza viruses.* Annu Rev Genet, 2002. **36**: p. 305-32.
9. Subbarao, K. and T. Joseph, *Scientific barriers to developing vaccines against avian influenza viruses.* Nat Rev Immunol, 2007. **7**(4): p. 267-78.
10. Hilleman, M.R., *Realities and enigmas of human viral influenza: pathogenesis, epidemiology and control.* Vaccine, 2002. **20**(25-26): p. 3068-87.
11. Gerhard, W., *The role of the antibody response in influenza virus infection.* Curr Top Microbiol Immunol, 2001. **260**: p. 171-90.

12. Stephenson, I., et al., *Confronting the avian influenza threat: vaccine development for a potential pandemic.* Lancet Infect Dis, 2004. **4**(8): p. 499-509.
13. Lin, Y.P., et al., *Avian-to-human transmission of H9N2 subtype influenza A viruses: relationship between H9N2 and H5N1 human isolates.* Proc Natl Acad Sci U S A, 2000. **97**(17): p. 9654-8.
14. Kawaoka, Y., S. Krauss, and R.G. Webster, *Avian-to-human transmission of the PB1 gene of influenza A viruses in the 1957 and 1968 pandemics.* J Virol, 1989. **63**(11): p. 4603-8.
15. Scholtissek, C., et al., *On the origin of the human influenza virus subtypes H2N2 and H3N2.* Virology, 1978. **87**(1): p. 13-20.
16. Zambon, M.C., *The pathogenesis of influenza in humans.* Rev Med Virol, 2001. **11**(4): p. 227-41.
17. Shinya, K., et al., *Avian flu: influenza virus receptors in the human airway.* Nature, 2006. **440**(7083): p. 435-6.
18. van Riel, D., et al., *H5N1 Virus Attachment to Lower Respiratory Tract.* Science, 2006. **312**(5772): p. 399.
19. Ito, T., et al., *Molecular basis for the generation in pigs of influenza A viruses with pandemic potential.* J Virol, 1998. **72**(9): p. 7367-73.
20. Glaser, L., et al., *Effective replication of human influenza viruses in mice lacking a major alpha2,6 sialyltransferase.* Virus Res, 2007. **126**(1-2): p. 9-18.
21. Perdue, M.L., et al., *Virulence-associated sequence duplication at the hemagglutinin cleavage site of avian influenza viruses.* Virus Res, 1997. **49**(2): p. 173-86.
22. Pappas, C., et al., *Single gene reassortants identify a critical role for PB1, HA, and NA in the high virulence of the 1918 pandemic influenza virus.* Proc Natl Acad Sci U S A, 2008. **105**(8): p. 3064-9.

23. Van Hoeven, N., et al., *Human HA and polymerase subunit PB2 proteins confer transmission of an avian influenza virus through the air.* Proc Natl Acad Sci U S A, 2009. **106**(9): p. 3366-71.
24. Brammer, T.L., et al., *Surveillance for influenza--United States, 1997-98, 1998-99, and 1999-00 seasons.* MMWR Surveill Summ, 2002. **51**(7): p. 1-10.
25. Lui, K.J. and A.P. Kendal, *Impact of influenza epidemics on mortality in the United States from October 1972 to May 1985.* Am J Public Health, 1987. **77**(6): p. 712-6.
26. Patel, M., et al., *Pandemic (H1N1) 2009 influenza.* Br J Anaesth, 2010. **104**(2): p. 128-42.
27. Johnson, N.P. and J. Mueller, *Updating the accounts: global mortality of the 1918-1920 "Spanish" influenza pandemic.* Bull Hist Med, 2002. **76**(1): p. 105-15.
28. Simonsen, L., et al., *Pandemic versus epidemic influenza mortality: a pattern of changing age distribution.* J Infect Dis, 1998. **178**(1): p. 53-60.
29. WHO. *Pandemic (H1N1) 2009-update 70*. [cited 2009 October 20]; Available from: http://www.who.int/csr/don/2009_10_16/en/index.html.
30. Organization, W.H. *Preparing for the second wave: lessons from current outbreaks.* 2009; Available from: http://www.who.int/csr/disease/swineflu/notes/hlnl_second_wave_2009-828/en/index.html.
31. Baccam, P., et al., *Kinetics of influenza A virus infection in humans.* J Virol, 2006. **80**(15): p. 7590-9.
32. Tamura, S., T. Tanimoto, and T. Kurata, *Mechanisms of broad cross-protection provided by influenza virus infection and their application to vaccines.* Jpn J Infect Dis, 2005. **58**(4): p. 195-207.

33. Seo, S.H. and R.G. Webster, *Tumor necrosis factor alpha exerts powerful anti-influenza virus effects in lung epithelial cells.* J Virol, 2002. **76**(3): p. 1071-6.
34. Ada, G.L. and P.D. Jones, *The immune response to influenza infection.* Curr Top Microbiol Immunol, 1986. **128**: p. 1-54.
35. See, H. and P. Wark, *Innate immune response to viral infection of the lungs.* Paediatr Respir Rev, 2008. **9**(4): p. 243-50.
36. Charley, B., S. Riffault, and K. Van Reeth, *Porcine innate and adaptative immune responses to influenza and coronavirus infections.* Ann N Y Acad Sci, 2006. **1081**: p. 130-6.
37. Miettinen, M., et al., *IFNs activate toll-like receptor gene expression in viral infections.* Genes Immun, 2001. **2**(6): p. 349-55.
38. Tamura, S., H. Hasegawa, and T. Kurata, *Estimation of the effective doses of nasal-inactivated influenza vaccine in humans from mouse-model experiments.* Jpn J Infect Dis, 2010. **63**(1): p. 8-15.
39. Doherty, P.C., et al., *Effector CD4+ and CD8+ T-cell mechanisms in the control of respiratory virus infections.* Immunol Rev, 1997. **159**: p. 105-17.
40. Mosmann, T.R., et al., *T helper cytokine patterns: defined subsets, random expression, and external modulation.* Immunol Res, 2009.
41. Johansson, B.E., D.J. Bucher, and E.D. Kilbourne, *Purified influenza virus hemagglutinin and neuraminidase are equivalent in stimulation of antibody response but induce contrasting types of immunity to infection.* J Virol, 1989. **63**(3): p. 1239-46.
42. Black, R.A., et al., *Antibody response to the M2 protein of influenza A virus expressed in insect cells.* J Gen Virol, 1993. **74 (Pt 1)**: p. 143-6.

43. Murphy, B.R. and M.L. Clements, *The systemic and mucosal immune response of humans to influenza A virus.* Curr Top Microbiol Immunol, 1989. **146**: p. 107-16.
44. McHeyzer-Williams, M.G. and R. Ahmed, *B cell memory and the long-lived plasma cell.* Curr Opin Immunol, 1999. **11**(2): p. 172-9.
45. Takahashi, Y., *Memory B cells in systemic and mucosal immune response: implications for successful vaccination.* Biosci Biotechnol Biochem, 2007. **71**(10): p. 2358-66.
46. Slifka, M.K. and R. Ahmed, *Long-term humoral immunity against viruses: revisiting the issue of plasma cell longevity.* Trends Microbiol, 1996. **4**(10): p. 394-400.
47. Bachmann, M.F., et al., *Free recirculation of memory B cells versus antigen-dependent differentiation to antibody-forming cells.* J Immunol, 1994. **153**(8): p. 3386-97.
48. Joo, H.M., Y. He, and M.Y. Sangster, *Broad dispersion and lung localization of virus-specific memory B cells induced by influenza pneumonia.* Proc Natl Acad Sci U S A, 2008. **105**(9): p. 3485-90.
49. Gowans, J.L. and E.J. Knight, *The Route of Re-Circulation of Lymphocytes in the Rat.* Proc R Soc Lond B Biol Sci, 1964. **159**: p. 257-82.
50. Okada, T. and J.G. Cyster, *B cell migration and interactions in the early phase of antibody responses.* Curr Opin Immunol, 2006. **18**(3): p. 278-85.
51. Gonzalez, S.F., et al., *B cell acquisition of antigen in vivo.* Curr Opin Immunol, 2009. **21**(3): p. 251-7.
52. Miller, M.J., et al., *Two-photon imaging of lymphocyte motility and antigen response in intact lymph node.* Science, 2002. **296**(5574): p. 1869-73.

53. Pape, K.A., et al., *The humoral immune response is initiated in lymph nodes by B cells that acquire soluble antigen directly in the follicles.* Immunity, 2007. **26**(4): p. 491-502.
54. Roozendaal, R., et al., *Conduits mediate transport of low-molecular-weight antigen to lymph node follicles.* Immunity, 2009. **30**(2): p. 264-76.
55. Bergtold, A., et al., *Cell surface recycling of internalized antigen permits dendritic cell priming of B cells.* Immunity, 2005. **23**(5): p. 503-14.
56. Batista, F.D., et al., *The role of integrins and coreceptors in refining thresholds for B-cell responses.* Immunol Rev, 2007. **218**: p. 197-213.
57. Junt, T., et al., *Subcapsular sinus macrophages in lymph nodes clear lymph-borne viruses and present them to antiviral B cells.* Nature, 2007. **450**(7166): p. 110-4.
58. Phan, T.G., et al., *Subcapsular encounter and complement-dependent transport of immune complexes by lymph node B cells.* Nat Immunol, 2007. **8**(9): p. 992-1000.
59. Phan, T.G., et al., *Immune complex relay by subcapsular sinus macrophages and noncognate B cells drives antibody affinity maturation.* Nat Immunol, 2009. **10**(7): p. 786-93.
60. Rock, K.L., B. Benacerraf, and A.K. Abbas, *Antigen presentation by hapten-specific B lymphocytes. I. Role of surface immunoglobulin receptors.* J Exp Med, 1984. **160**(4): p. 1102-13.
61. Lanzavecchia, A., *Mechanisms of antigen uptake for presentation.* Curr Opin Immunol, 1996. **8**(3): p. 348-54.
62. Harwood, N.E. and F.D. Batista, *New insights into the early molecular events underlying B cell activation.* Immunity, 2008. **28**(5): p. 609-19.

63. Jacob, J., R. Kassir, and G. Kelsoe, *In situ studies of the primary immune response to (4-hydroxy-3-nitrophenyl)acetyl. I. The architecture and dynamics of responding cell populations.* J Exp Med, 1991. **173**(5): p. 1165-75.
64. Liu, Y.J., et al., *Sites of specific B cell activation in primary and secondary responses to T cell-dependent and T cell-independent antigens.* Eur J Immunol, 1991. **21**(12): p. 2951-62.
65. Gulbranson-Judge, A. and I. MacLennan, *Sequential antigen-specific growth of T cells in the T zones and follicles in response to pigeon cytochrome c.* Eur J Immunol, 1996. **26**(8): p. 1830-7.
66. Luther, S.A., et al., *Viral superantigen drives extrafollicular and follicular B cell differentiation leading to virus-specific antibody production.* J Exp Med, 1997. **185**(3): p. 551-62.
67. Sze, D.M., et al., *Intrinsic constraint on plasmablast growth and extrinsic limits of plasma cell survival.* J Exp Med, 2000. **192**(6): p. 813-21.
68. Allen, C.D., T. Okada, and J.G. Cyster, *Germinal-center organization and cellular dynamics.* Immunity, 2007. **27**(2): p. 190-202.
69. Allen, C.D. and J.G. Cyster, *Follicular dendritic cell networks of primary follicles and germinal centers: phenotype and function.* Semin Immunol, 2008. **20**(1): p. 14-25.
70. Vinuesa, C.G., et al., *Follicular B helper T cells in antibody responses and autoimmunity.* Nat Rev Immunol, 2005. **5**(11): p. 853-65.
71. Bishop, G.A. and B.S. Hostager, *B lymphocyte activation by contact-mediated interactions with T lymphocytes.* Curr Opin Immunol, 2001. **13**(3): p. 278-85.
72. Stavnezer, J., *Immunology. A touch of antibody class.* Science, 2000. **288**(5468): p. 984-5.

73. Banchereau, J. and R.M. Steinman, *Dendritic cells and the control of immunity.* Nature, 1998. **392**(6673): p. 245-52.
74. Klein, J. and N. Takahata, *The major histocompatibility complex and the quest for origins.* Immunol Rev, 1990. **113**: p. 5-25.
75. Crowe, S.R., et al., *Uneven distribution of MHC class II epitopes within the influenza virus.* Vaccine, 2006. **24**(4): p. 457-67.
76. Bui, H.H., et al., *Ab and T cell epitopes of influenza A virus, knowledge and opportunities.* Proc Natl Acad Sci U S A, 2007. **104**(1): p. 246-51.
77. Richards, K.A., et al., *Direct ex vivo analyses of HLA-DR1 transgenic mice reveal an exceptionally broad pattern of immunodominance in the primary HLA-DR1-restricted CD4 T-cell response to influenza virus hemagglutinin.* J Virol, 2007. **81**(14): p. 7608-19.
78. Recher, M., et al., *Deliberate removal of T cell help improves virus-neutralizing antibody production.* Nat Immunol, 2004. **5**(9): p. 934-42.
79. Sangster, M.Y., et al., *Analysis of the virus-specific and nonspecific B cell response to a persistent B-lymphotropic gammaherpesvirus.* J Immunol, 2000. **164**(4): p. 1820-8.
80. Woods, A., et al., *Human major histocompatibility complex class II-restricted T cell responses in transgenic mice.* J Exp Med, 1994. **180**(1): p. 173-81.
81. Yamamoto, K., et al., *Functional interaction between human histocompatibility leukocyte antigen (HLA) class II and mouse CD4 molecule in antigen recognition by T cells in HLA-DR and DQ transgenic mice.* J Exp Med, 1994. **180**(1): p. 165-71.
82. Rosloniec, E.F., et al., *An HLA-DR1 transgene confers susceptibility to collagen-induced arthritis elicited with human type II collagen.* J Exp Med, 1997. **185**(6): p. 1113-22.

83. Richards, K.A., F.A. Chaves, and A.J. Sant, *Infection of HLA-DR1 transgenic mice with a human isolate of influenza a virus (H1N1) primes a diverse CD4 T-cell repertoire that includes CD4 T cells with heterosubtypic cross-reactivity to avian (H5N1) influenza virus.* J Virol, 2009. **83**(13): p. 6566-77.
84. Wood, J.M., *Selection of influenza vaccine strains and developing pandemic vaccines.* Vaccine, 2002. **20 Suppl 5**: p. B40-4.
85. Doherty, P.C., et al., *Dissecting the host response to a gamma-herpesvirus.* Philos Trans R Soc Lond B Biol Sci, 2001. **356**(1408): p. 581-93.
86. Hamilton-Easton, A. and M. Eichelberger, *Virus-specific antigen presentation by different subsets of cells from lung and mediastinal lymph node tissues of influenza virus-infected mice.* J Virol, 1995. **69**(10): p. 6359-66.
87. Lopez, C.B., et al., *A mouse model for immunization with ex vivo virus-infected dendritic cells.* Cell Immunol, 2000. **206**(2): p. 107-15.
88. Woodland, D.L. and T.D. Randall, *Anatomical features of anti-viral immunity in the respiratory tract.* Semin Immunol, 2004. **16**(3): p. 163-70.
89. Kedl, R.M., J.W. Kappler, and P. Marrack, *Epitope dominance, competition and T cell affinity maturation.* Curr Opin Immunol, 2003. **15**(1): p. 120-7.
90. MacDonald, A.S., et al., *Cutting edge: Th2 response induction by dendritic cells: a role for CD40.* J Immunol, 2002. **168**(2): p. 537-40.
91. Ekkens, M.J., et al., *The role of OX40 ligand interactions in the development of the Th2 response to the gastrointestinal nematode parasite Heligmosomoides polygyrus.* J Immunol, 2003. **170**(1): p. 384-93.
92. Garside, P., et al., *Visualization of specific B and T lymphocyte interactions in the lymph node.* Science, 1998. **281**(5373): p. 96-9.

93. Takahashi, Y., et al., *In situ studies of the primary immune response to (4-hydroxy-3-nitrophenyl)acetyl. V. Affinity maturation develops in two stages of clonal selection.* J Exp Med, 1998. **187**(6): p. 885-95.
94. Nayak, J.L., et al., *Analyses of the specificity of CD4 T cells during the primary immune response to influenza virus reveals dramatic MHC-linked asymmetries in reactivity to individual viral proteins.* Viral Immunol, 2010. **23**(2): p. 169-80.
95. Dogan, I., et al., *Multiple layers of B cell memory with different effector functions.* Nat Immunol, 2009. **10**(12): p. 1292-9.
96. Reinhardt, R.L., H.E. Liang, and R.M. Locksley, *Cytokine-secreting follicular T cells shape the antibody repertoire.* Nat Immunol, 2009. **10**(4): p. 385-93.
97. Cannons, J.L., et al., *SAP regulates T cell-mediated help for humoral immunity by a mechanism distinct from cytokine regulation.* J Exp Med, 2006. **203**(6): p. 1551-65.
98. Suzuki, K., et al., *Visualizing B cell capture of cognate antigen from follicular dendritic cells.* J Exp Med, 2009. **206**(7): p. 1485-93.
99. Hannum, L.G., et al., *Germinal center initiation, variable gene region hypermutation, and mutant B cell selection without detectable immune complexes on follicular dendritic cells.* J Exp Med, 2000. **192**(7): p. 931-42.

APPENDIX

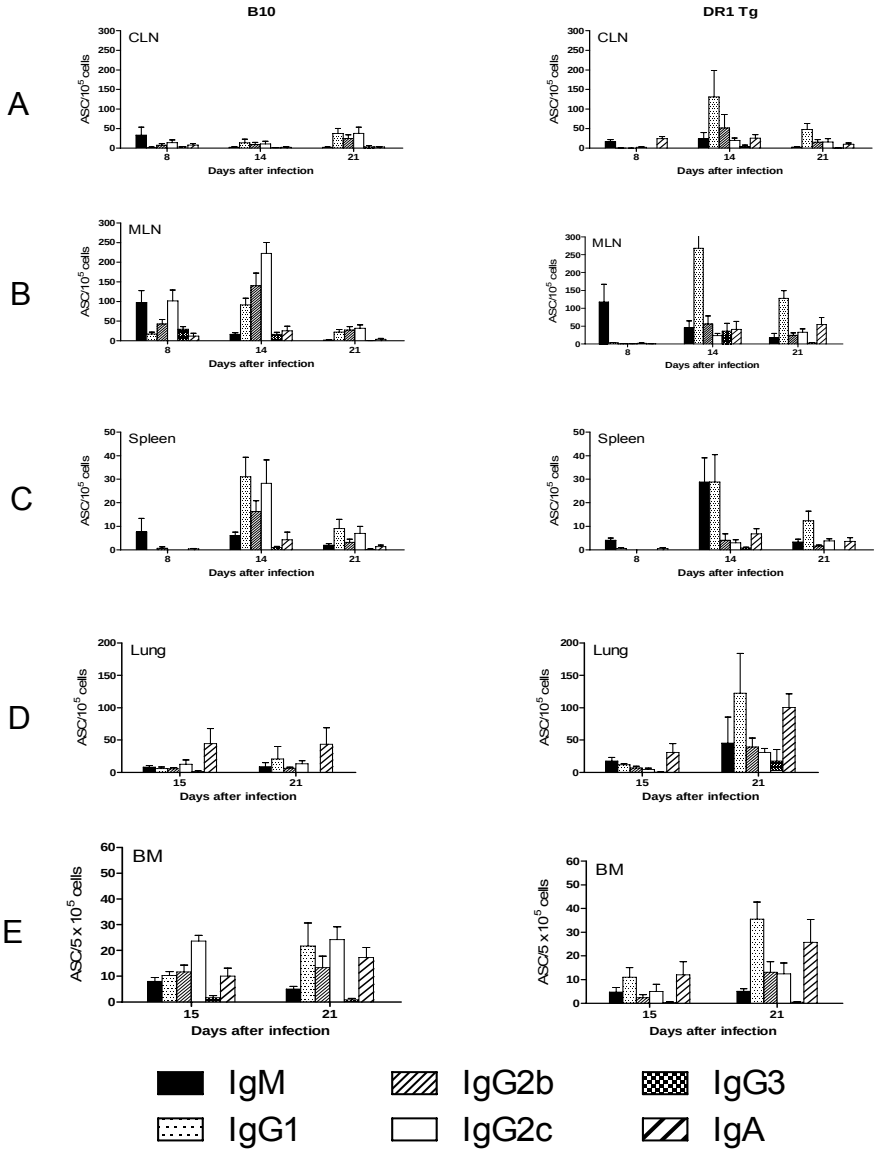

Figure 1. The primary influenza-specific ASCs response to intranasal administration of NC in DR1 Tg mice and B10 mice

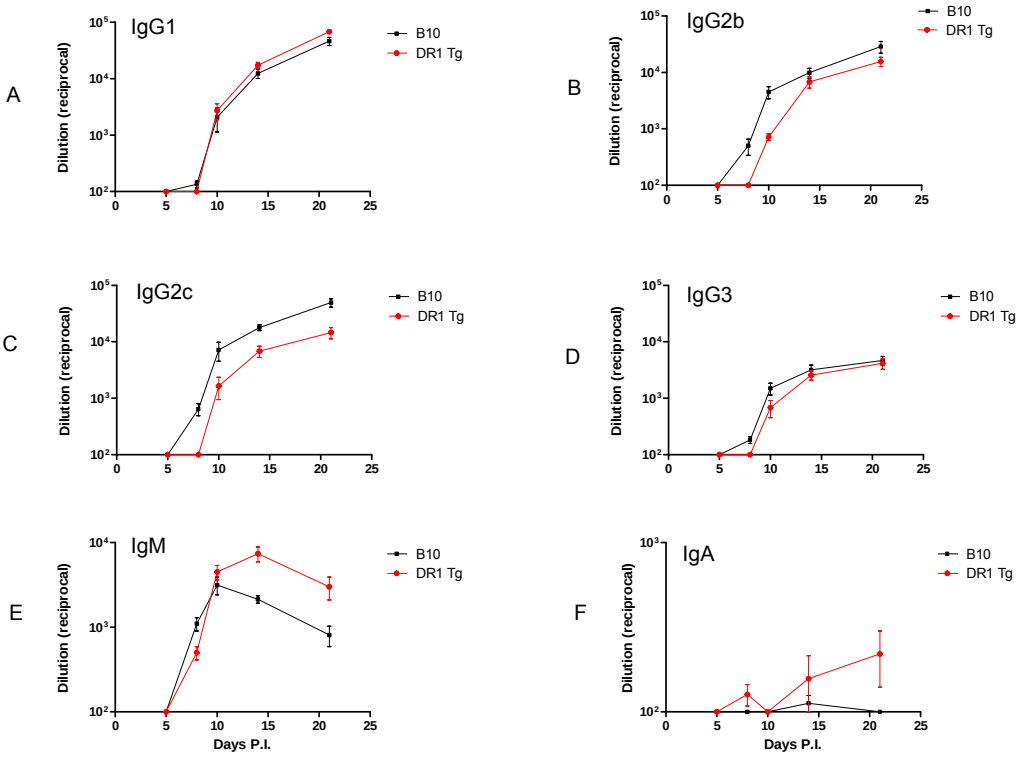

Figure 2. The influenza-specific Abs level in serum after intranasal administration of NC in DR1 Tg mice and B10 mice

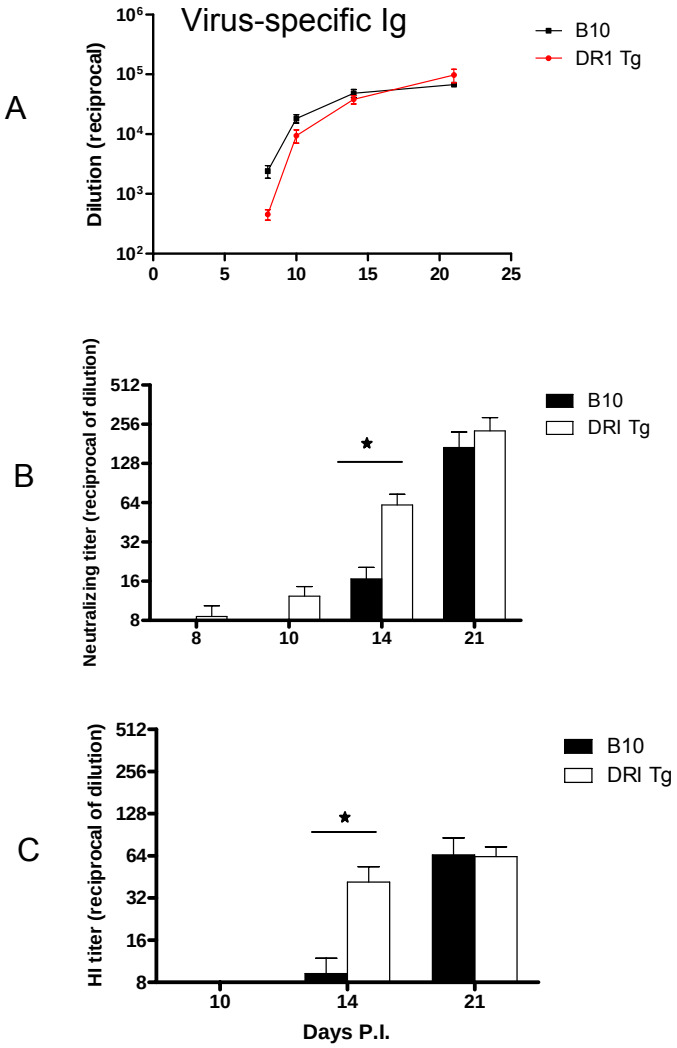

Figure 3. The influenza-specific immunoglobulin level and neutralizing Abs titers and hemagglutination inhibition titers in serum after intranasal administration

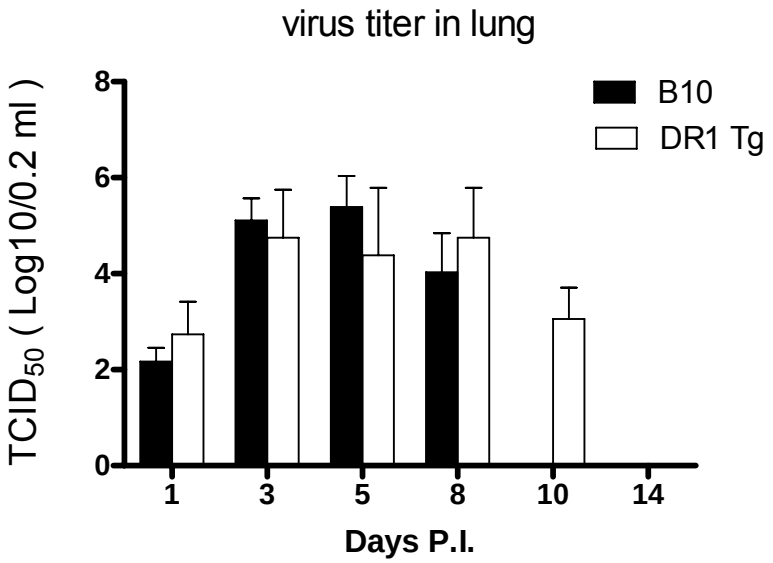

Figure 4. Virus replication in the lung after intranasal infection of NC in DR1 Tg mice and B10 mice

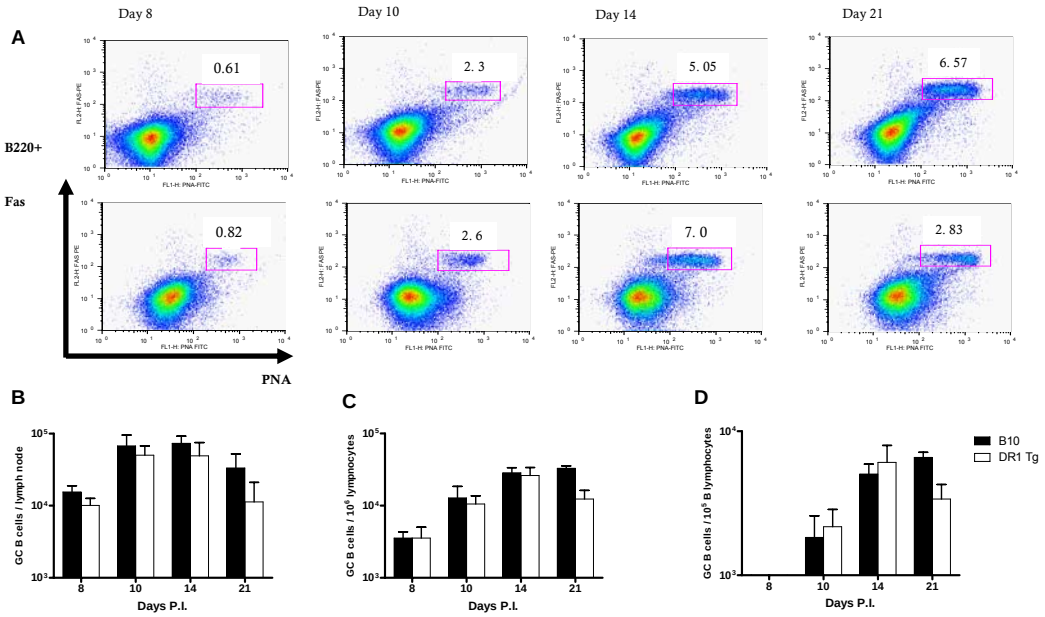

Figure 5. Germinal center formation in the MLN of DR1 Tg mice and B10 mice after i.n. NC infection

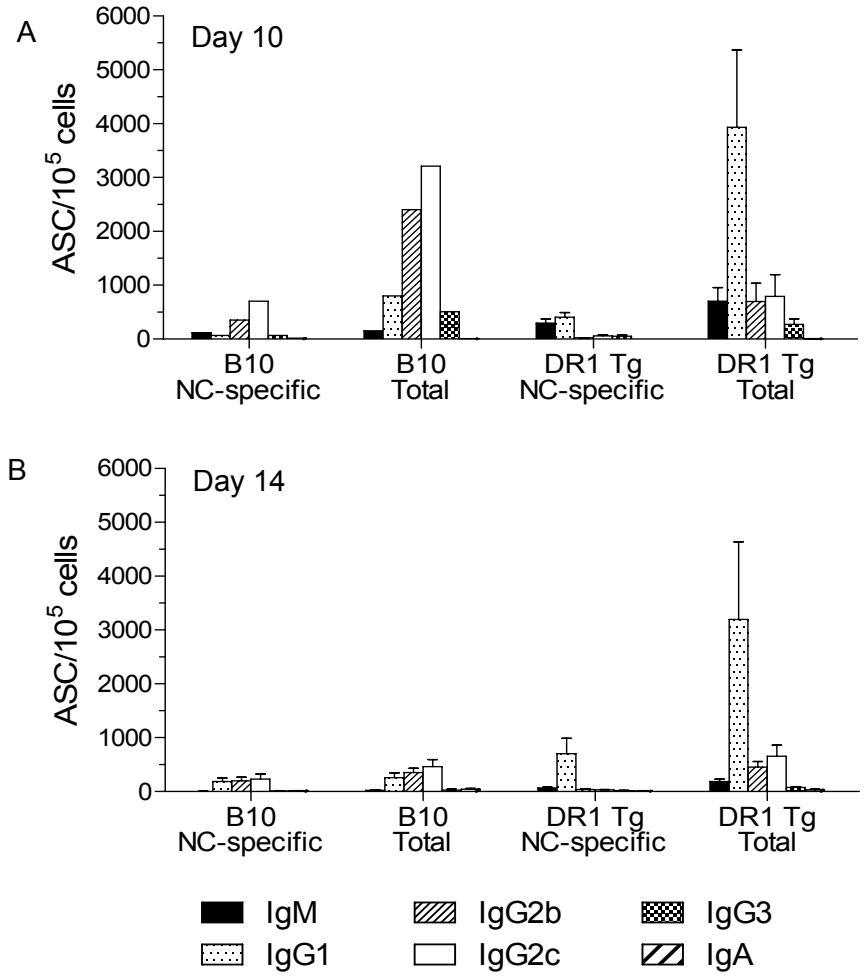

Figure 6. Comparison of influenza-specific and non-specific ASCs responses in the MLN of DR1 Tg mice and B10 mice following intranasal infection of NC

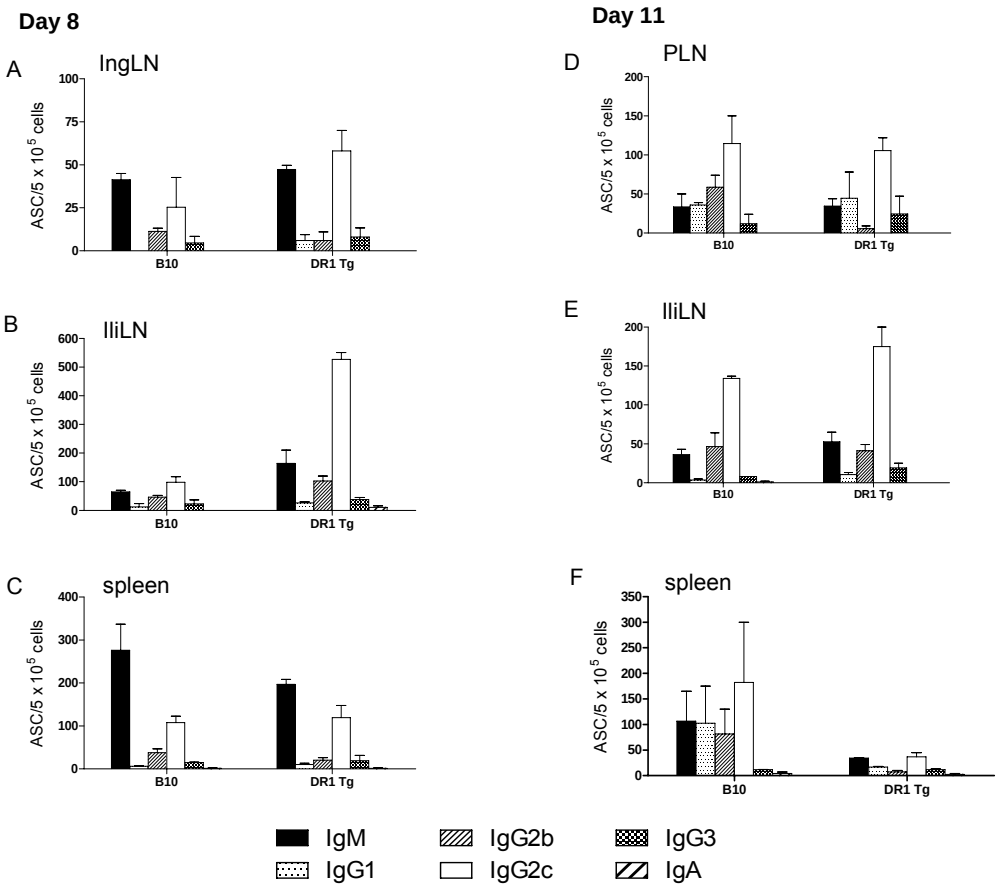

Figure 7. The primary influenza-specific ASCs response to intramuscular administration of inactivated NC in DR1 Tg mice and B10 mice

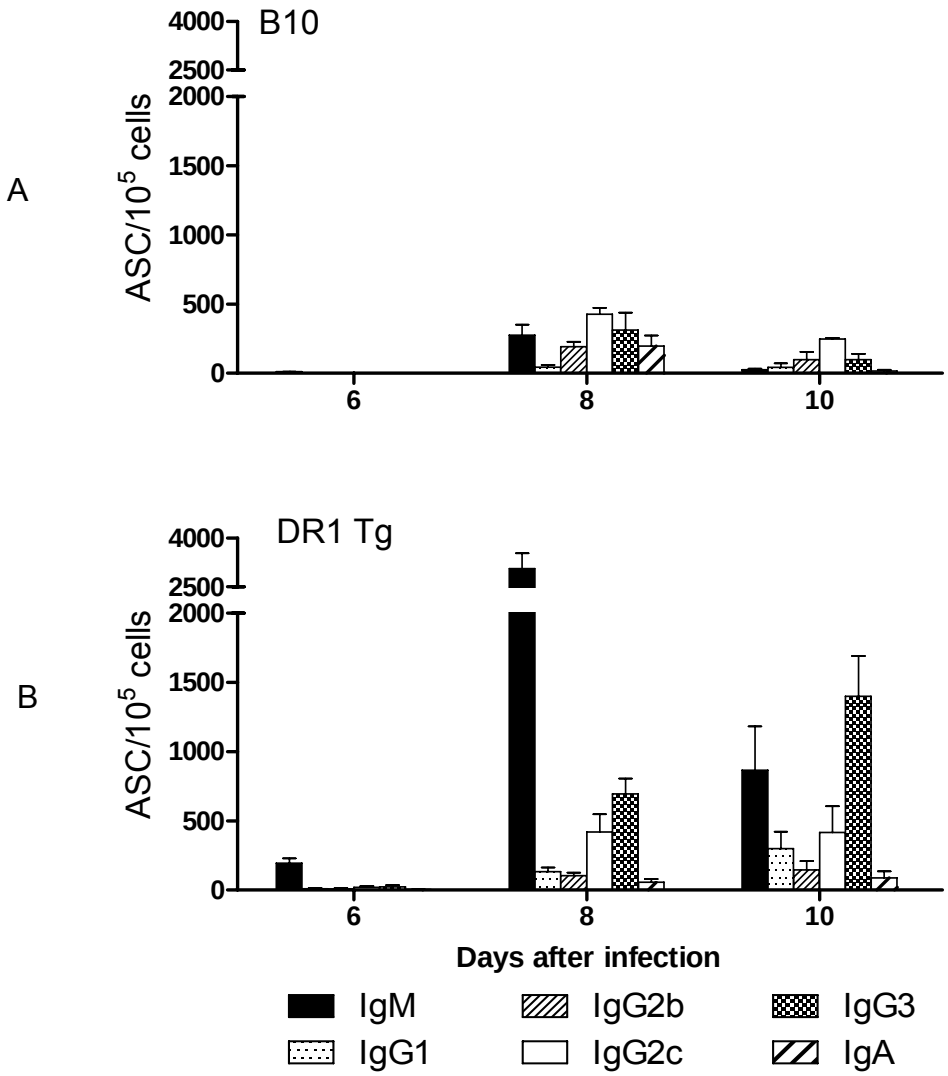

Figure 8. The influenza-specific ASCs response to intranasal administration of influenza virus PR8 in DR1 Tg mice and B10 mice

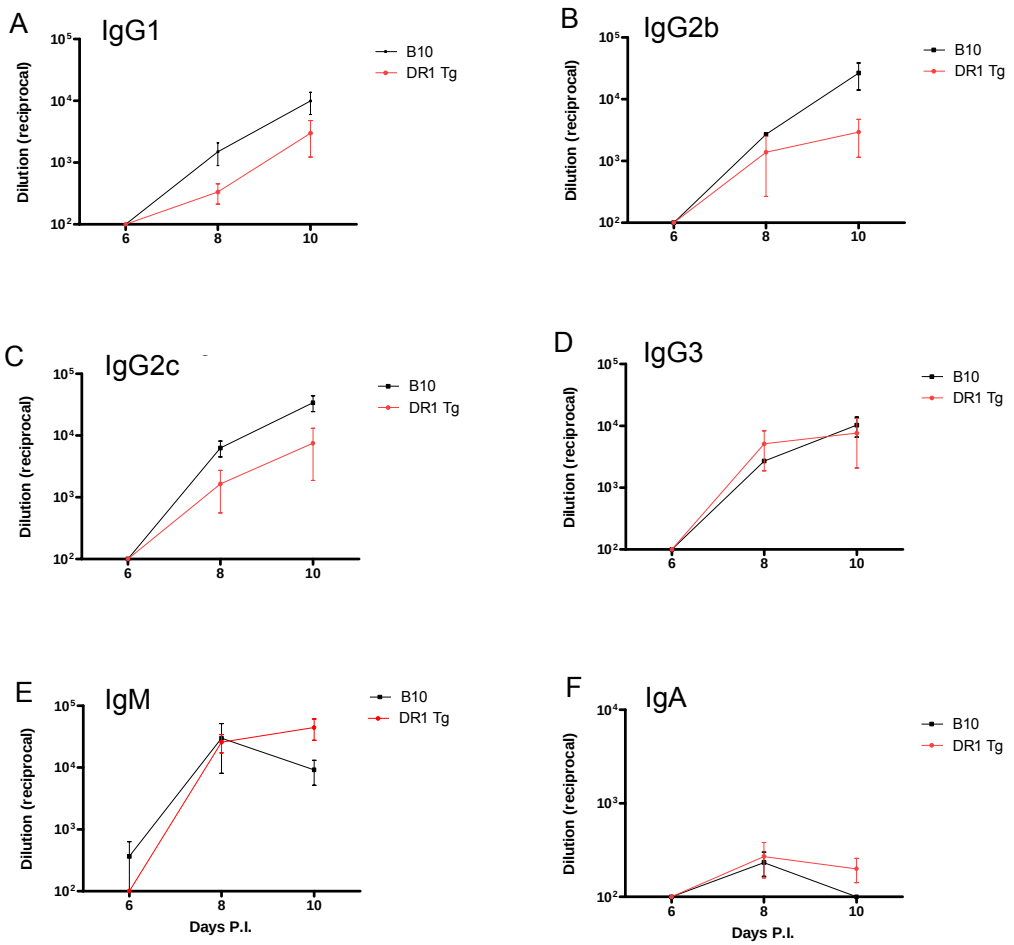

Figure 9. Influenza-specific Abs levels in serum after intranasal infection of PR8 in DR1 Tg mice and B10 mice

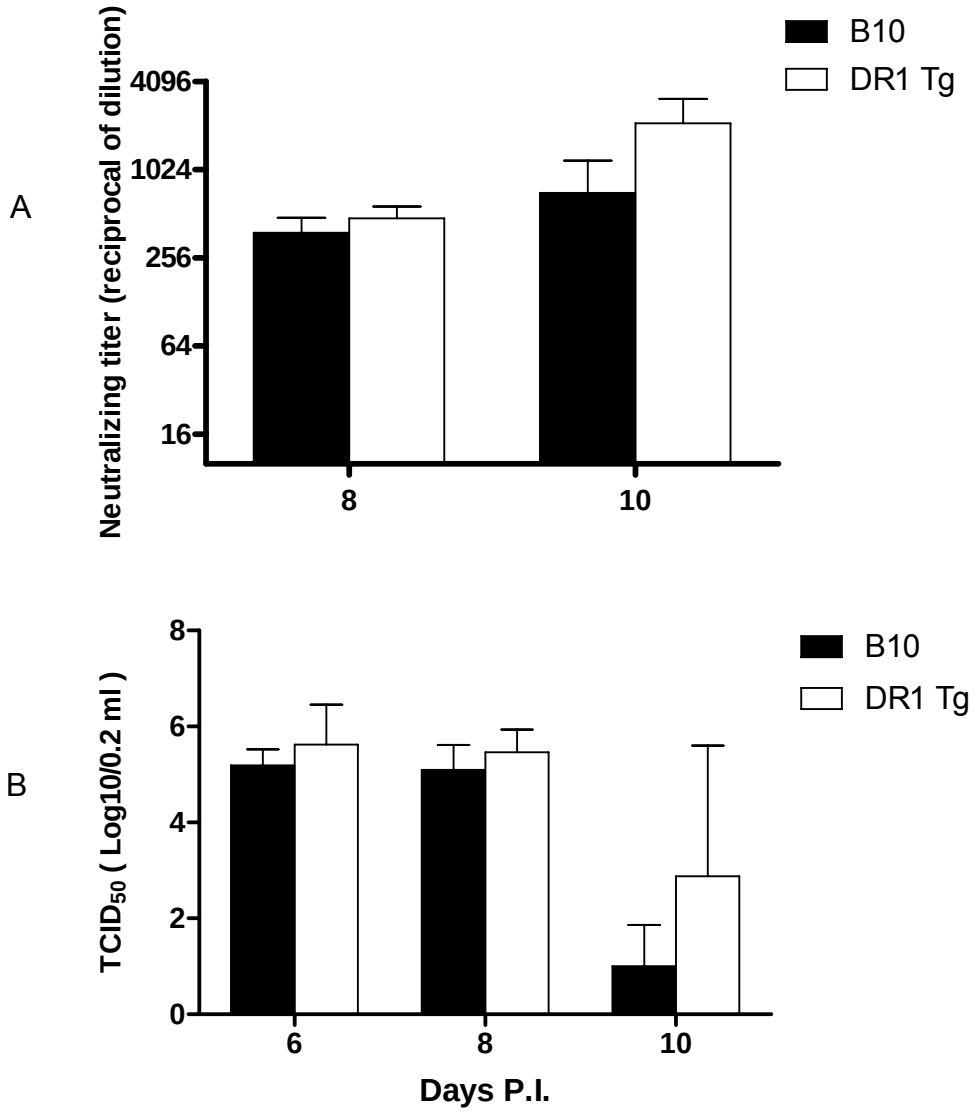

Figure 10. Neutralizing Abs titers in serum and viral growth in the lung after intranasal infection of PR8 in DR1 Tg mice and B10 mice

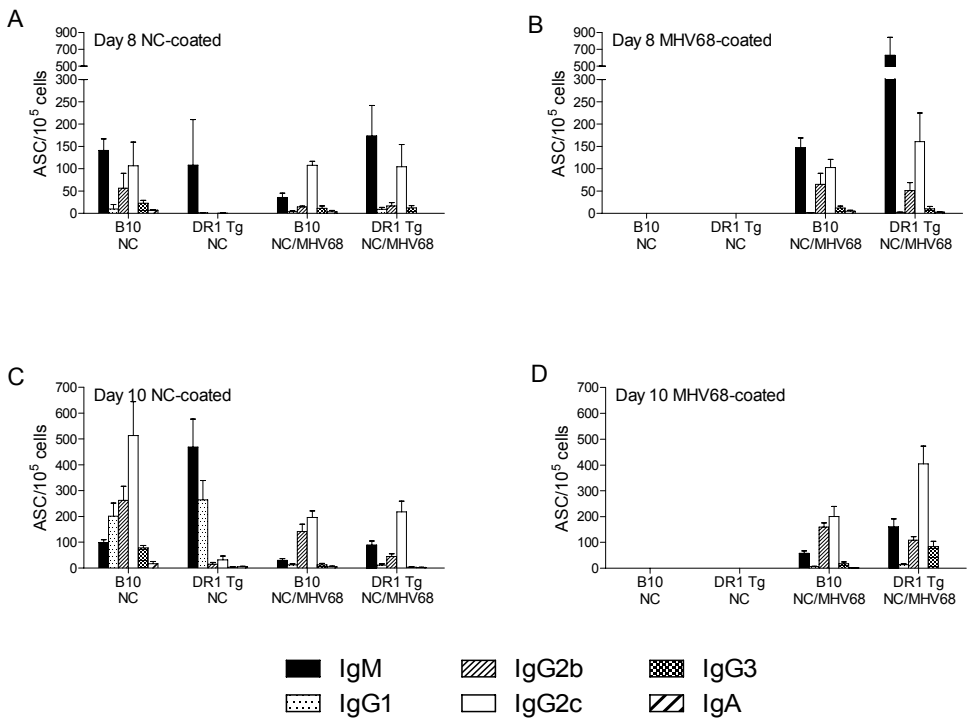

Figure 11. Influenza-specific ASCs responses in mice co-infected with NC and MHV-68 viruses

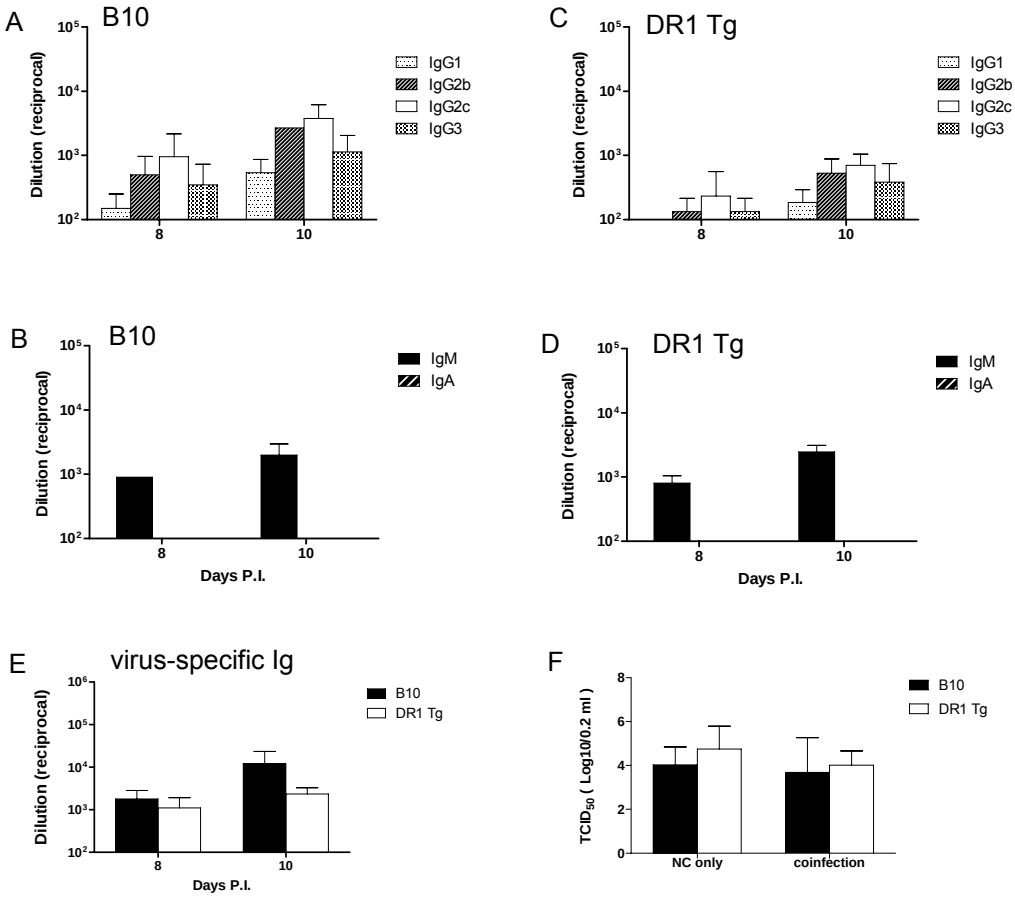

Figure 12. Influenza-specific Abs levels in serum of mice co-infected with NC and MHV-68 viruses

Vita

Lifang Huan was born on July 24th, 1982 in Shandong, China. She graduated from Shandong University 2004 and received her B.S degree majoring in public health. She attended China CDC for her Master study between 2004-2007 and graduated with M.S degree with the major of pathogenic biology. She began her graduate study at the University of Tennessee, Knoxville in Fall 2007. She graduated with a Master degree in Microbiology in the summer of 2010.